2019

Baryons in a light front approach

Anji Yu
Iowa State University

Baryons in a light front approach

by

Anji Yu

A thesis submitted to the graduate faculty

in partial fulfillment of the requirements for the degree of

MASTER OF SCIENCE

Major: Physics

Program of Study Committee:
James P. Vary, Major Professor
Pieter Maris
Jigang Wang
Sung-Yell Song
Pavankumar R Aduri

The student author, whose presentation of the scholarship herein was approved by the program of study committee, is solely responsible for the content of this thesis. The Graduate College will ensure this thesis is globally accessible and will not permit alterations after a degree is conferred.

Iowa State University

Ames, Iowa

2019

DEDICATION

This thesis is dedicated to my parents.

TABLE OF CONTENTS

Page

ACKNOWLEDGMENTS

I would first like to thank my advisor, Prof. James P. Vary, Ph.D. He has always been patient and encouraging. He consistently allows me to explore the area that interested me but steers me in the right direction whenever he thinks I need it. I would like to thank Yang Li, Ph.D. His solid understanding of physics and mathematics makes him a great researcher and mentor. He is talented, diligent, and most importantly, passionate. I can always get encouraged by him. I also wish to thank Prof. Pieter Maris, Ph.D. He can always provide insightful advice.

I would like to express my appreciations to other committee members Prof. Sung-Yell Song, Ph.D., Prof. Jigang Wang, Ph.D., Prof. Pavan Aduri, Ph.D..

Finally, I would like to thank all those who helped me in various ways for these years in Iowa State University.

ABSTRACT

We present a model for baryons based on three constituent quarks using light-front holography together with basis light-front quantization (BLFQ). The work is generalized from the method which originally developed for meson systems using a constituent quark and an antiquark. We construct an effective 3-body Hamiltonian, which consists of a transverse confining interaction based on the Ads/QCD soft-wall model, and a longitudinal confining interaction which was first applied to mesons. We employ this model for the proton by calculating its form factor $F_1(q^2)$. The results are compared with experimental measurements and other theoretical methods. We develop generalized Jacobi coordinates, as well as a generalized longitudinal confinement, that will enable this model to be generalized to systems with more than three constituent quarks.

CHAPTER 1. LIGHT-FRONT QUANTIZATION

1.1 Background

In classical physics, the physical laws are often stated and studied in the lab frame, which is a special frame of reference and assumed to be static. Isaac Newton discovered the celebrated "Newton's laws of motion", which revealed the relation between force and motion. Newton emphasized the vector aspects of motions and his theory is usually referred as Newtonian mechanics. Under the same scheme, it was proven that the physical laws are invariant under a group of transformations called the Galilean transformation group [1].

Later, researchers started to realize that there are equivalent formulations of classical mechanics, by which physical laws can be stated in terms of scalars. This idea promotes classical mechanics to another level which is categorized as analytical mechanics. The two most famous and widely adopted formalisms among them are Lagrangian mechanics and Hamiltonian mechanics, which are founded and named after Joseph-Louis Lagrange and William Rowan Hamilton, respectively.

Lagrangian mechanics reformulates classical mechanics in distinct ways. In Newtonian mechanics, physical laws are described in certain Cartesian coordinates called Galilean coordinates [1], while Lagrangian mechanics describes motion by means of the configuration space. The scalar in which physical laws are encoded is now called the Lagrangian (L), which is a function of coordinates living in configuration space called generalized coordinates and their time derivatives called generalized velocities (and possibly with time). The equations which describe motion are called Euler-Lagrange equations of motion.

Hamiltonian mechanics is developed from Lagrangian mechanics, but uses a different mathematical formalism. Instead of configuration space, Hamiltonian mechanics describes motions in a phase space, employs canonical coordinate pairs to describe motion. Phase space is defined in terms of pairs of generalized coordinates and momenta that are related though having a Poisson

bracket which is unity. The equations of motion in phase space are differential equations acting on a scalar called the Hamiltonian (H). The Hamilton's equations of motion have a built-in symplectic structure, revealing the natural symplectic structure setting in classical mechanics; it also has great value for approximation methods in perturbation theory. The two scalars L and H are related by a Legendre transformation.

Over time, the original formulations of classical mechanics became challenged by increasingly precise experiments. One of those significant discoveries in the twentieth century occurred when Galilean symmetry failed to explain the experimental fact that the speed of light "c" is the same in any frame of reference. In other words, the physical laws are no longer invariant under Galilean transformations. Although Newtonian mechanics is still powerful and useful since Newton's laws hold rather well in the non-relativistic limit where all velocities are small compared to the speed of light, researchers sought for improved descriptions that work for systems with arbitrary velocities. Ultimately, Albert Einstein proposed a brand new theory, the well-known theory of relativity. In his relativity point of view, time and space are merged together into 4-dimensional (4D) space-time. Many scientists struggled to overcome their classical (Newtonian) instincts to accept the relativity theory, since it was not straightforward to generalize Newtonian mechanics to a relativistic theory. However, both the Lagrangian and Hamiltonian formulations were more easily adapted to a relativistic theory and this led researchers to concentrate their efforts on these formulations.

Another innovation in the same period of time was the birth of quantum mechanics, which aims to describe the behavior of systems on a microscopic scale. It is a theory that explains experimental phenomena in terms of probabilities and relates particles to waves by a constant $\hbar$ called reduced Planck's constant. Not surprisingly, there are formulations of quantum mechanics adopting the Lagrangian and the Hamiltonian approaches. The evolution of the system could be described by Schrödinger equation based on the Hamiltonian approach, or the path integral which adopts the Lagrangian approach. Quantum systems are usually complicated, hence applications using perturbation theory based either on the Hamiltonian approach (e.g. time-dependent perturbation

theory) or the Lagrangian approach (covariant perturbation theory) play a huge role in the theory of quantum mechanics.

The two theories have been brilliantly coalesced into what is called quantum field theory (QFT) [2]. Our work is to model the behavior of elementary particles, based on QFT.

We adopt natural units, i.e., $c = \hbar = 1$ throughout the thesis.

1.2 Lorentz transformation

In relativity, the physical laws are invariant under the Poincaré transformation, which is also known as the inhomogeneous Lorentz transformation. The Poincaré transformation for the space-time vector $x^\mu \equiv (x^0, x^1, x^2, x^3) = (t, \boldsymbol{x})$ is

$$x'^\mu = \Lambda^\mu_\nu x^\nu + a^\mu, \tag{1.1}$$

where Λ is the homogeneous part, known as Lorentz transformation matrix, and $\mu, \nu = 0, 1, 2, 3$ are space-time indices. The index ν on the right-hand side of Eq.(1.1) appears in pairs and is summed over 0 to 3 according to Einstein summation convention. We adopt this convention throughout this thesis unless otherwise stated. The Lorentz transformation group preserves the Minkowski metric tensor $g_{\mu\nu}$ in the sense that

$$\Lambda^\mu_\sigma \Lambda^\nu_\rho g_{\mu\nu} = g_{\sigma\rho}, \tag{1.2}$$

where $g_{\mu\nu}$ is given by

$$g_{\mu\nu} = g^{\mu\nu} = \begin{pmatrix} +1 & 0 & 0 & 0 \\ 0 & -1 & 0 & 0 \\ 0 & 0 & -1 & 0 \\ 0 & 0 & 0 & -1 \end{pmatrix}. \tag{1.3}$$

Hence one can see the Lorentz transformations form the group $\mathrm{L} \equiv \mathrm{O}(3,1)$. Meanwhile, the inhomogeneous part which serves as translations also form a group $\mathrm{T} \equiv \mathbb{R}^{1,3} \cong \mathbb{R}^4$, and is invariant under Lorentz transformation (by conjugation). The two subgroups generate the Poincaré transformation group P and intersect trivially. Therefore, P is a semidirect product of its two components, written as $\mathrm{P} \equiv \mathrm{T} \rtimes \mathrm{L}$ when there is no ambiguity.

Quantum mechanics postulates that the system is described by a state, which is a set of equivalence class of nonzero vectors in the Hilbert space over complex number field $\mathbb{C}$ where the equivalence relation is given by scalar multiplication. When there is no ambiguity the state also refers to a unit representative (a vector with unit norm). The experimental observables are hermitian operators and the transformation between states is implemented by applying unitary operators. In the matrix sense, the unitary transformation is always obtained by taking exponential on some anti-hermitian operators, i.e., observables multiplied by imaginary unit "i". The representation of a state $|\psi\rangle$ on a complete set of basis in the Hilbert space is called the wave function with respect to that basis, and the basis are usually eigenvectors of some observables of unit length, i.e., they are orthonormal. The continuous transformation group in a Hilbert space possesses a manifold structure, they are always Lie groups associated with an underlying Lie algebra which is an vector space closed under Lie bracket. In the matrix sense, the Lie bracket is matrix commutator. Any set of basis of the Lie algebra is called a set of generators of the corresponding Lie group.

To study how a transformation acts on a state, sometimes it is easier to study how the underlying algebra acts on states, then passes the action to the group by their correspondence, which is usually an exponential map. The overall motivation is that it is equivalent to study the group as well as the algebra, but it is far easier to study the algebra first then apply results to the group.

The Poincaré transformation group has ten generators, with four from T and six from L. The algebra generated by them is called Poincaré algebra. They are defined by the commutator relation

$$\begin{aligned} [P^\mu, P^\nu] &= 0 \\ [P^\mu, M^{\alpha\beta}] &= \mathrm{i}(g^{\mu\alpha}P^\beta - g^{\mu\beta}P^\alpha) \\ [M^{\mu\nu}, M^{\rho\sigma}] &= \mathrm{i}(g^{\mu\sigma}M^{\nu\rho} - g^{\nu\sigma}M^{\mu\rho} + g^{\nu\rho}M^{\mu\sigma} - g^{\mu\rho}M^{\nu\sigma}), \end{aligned} \tag{1.4}$$

where $\boldsymbol{P}$ is the 4-momentum operator from T, $\boldsymbol{M}$ are linear combinations of three boost and three angular momentum over $\mathbb{R}$ from L. The semidirect product structure of the Poincaré group is naturally carried over to the Poincaré algebra, in particular, the subalgebra generated by the momentum operator $\boldsymbol{P}$ is an abelian algebra of dimension 4, i.e., $\boldsymbol{P}$ are mutually commuting set, hence share common eigenvectors, $P^\mu |p^\mu\rangle = p^\mu |p^\mu\rangle$. For a single particle state $|\phi\rangle$, by acting on

$\boldsymbol{P}^2$ with it one should get

$$\boldsymbol{P}^2 \left|\phi\right\rangle = \boldsymbol{p}^2 \left|\phi\right\rangle = m^2 \left|\phi\right\rangle, \tag{1.5}$$

where m is the mass of the particle. This will be the starting point of our model.

1.3 Light-Front Dynamics

Non-relativistic quantum mechanics postulates that, the dynamics of a system is described by a quantum state $|\psi(t)\rangle$, which evolves according to the Schrödinger equation

$$\mathrm{i}\frac{\partial}{\partial t}\left|\psi(t)\right\rangle = \hat{H}\left|\psi(t)\right\rangle, \tag{1.6}$$

where $\hat{H}$ is the Hamiltonian operator of the system, and is quantized at the constant time t. However, in relativity, time and space coordinates are placed on an equal footing, which provides options to quantize the system in different forms and light-front quantization is one of them.

For any 4-vector $v^\mu = (v^0, v^1, v^2, v^3) \equiv (v^0, \boldsymbol{v})$, the light-front parametrization is defined as

$$(v^+, v^-, v^1, v^2) \equiv (v^0 + v^3, v^0 - v^3, v^1, v^2). \tag{1.7}$$

In particular, the light-front coordinates and momenta are,

$$\begin{aligned}(x^+, x^-, x^1, x^2) &= (x^0 + x^3, x^0 - x^3, x^1, x^2),\\ (p^+, p^-, p^1, p^2) &= (p^0 + p^3, p^0 - p^3, p^1, p^2).\end{aligned} \tag{1.8}$$

In terms of light-front parametrization, (x^+, p^-), (x^-, p^+), and $(\boldsymbol{x}^\perp, \boldsymbol{p}^\perp)$ are conjugate pairs (not canonical though). The metric tensor in the light-front dynamics is,

$$g_{\mu\nu} = \begin{pmatrix} 0 & \frac{1}{2} & 0 & 0 \\ \frac{1}{2} & 0 & 0 & 0 \\ 0 & 0 & -1 & 0 \\ 0 & 0 & 0 & -1 \end{pmatrix}, \qquad g^{\mu\nu} = \begin{pmatrix} 0 & 2 & 0 & 0 \\ 2 & 0 & 0 & 0 \\ 0 & 0 & -1 & 0 \\ 0 & 0 & 0 & -1 \end{pmatrix}, \tag{1.9}$$

where μ and ν take the order of $(+, -, 1, 2)$. Notice that the metric tensor is not diagonal as in the instant form shown in Eq.(1.3) above. The product of two 4-vectors $a \cdot b$ can be written as

$$a \cdot b \equiv a^\mu b_\mu = \frac{1}{2}a^+ b^- + \frac{1}{2}a^- b^+ - \boldsymbol{a}^\perp \cdot \boldsymbol{b}^\perp, \tag{1.10}$$

in the light-front scheme. In particular, the modulus squared of a 4-vector v is $|v|^2 = v^+v^- - \boldsymbol{v}_\perp^2$. Since in the transverse direction, we have $\boldsymbol{a}^\perp = -\boldsymbol{a}_\perp$, therefore $(\boldsymbol{a}^\perp)^2 = \boldsymbol{a}_\perp^2$. For the sake of convenience in typesetting, we uniformly adopt the subscript for "$\perp$" which should also help avoid confusion.

Similar to the equal-time quantization (or instant form) which is quantized at the regular time t, the light-front quantization is quantized at the light-front time x^+, and evolves according to the light-front Schrödinger equation [3]

$$\mathrm{i}\frac{\partial}{\partial x^+}\left|\psi(x^+)\right\rangle = \frac{1}{2}\hat{P}^-\left|\psi(x^+)\right\rangle, \tag{1.11}$$

where $\hat{P}^-$ is the conjugate momentum of the light-front time x^+, which serves as light-front Hamiltonian. Meanwhile, if the Lagrangian does not depend on the light-front time explicitly, then Eq.(1.11) is reduced to a time-independent equation

$$P_h^-\left|\psi\right\rangle = \frac{1}{2}\hat{P}^-\left|\psi\right\rangle, \tag{1.12}$$

where P_h^- is the eigenvalue of the equation. From the standpoint of matrix mechanics, solving this equation is equivalent to diagonalizing the Hamiltonian matrix; while from the function point of view, it is equivalent to solving a Sturm–Liouville problem. If the Hamiltonian describes a free particle, one has the dispersion relation $P^\mu P_\mu = M^2$. Therefore, in the light-front framework,

$$P_h^- = \frac{\boldsymbol{P}_\perp^2 + M^2}{2P^+}, \tag{1.13}$$

where M is the physical mass of the particle. Different from the equal-time dispersion relation, the light-front dispersion relation is linear in light-front time and quadratic in the transverse momenta. With the light-front (LF) Lorentz-invariant Hamiltonian $H_{LF} = P^+P^- - \boldsymbol{P}_\perp^2$, the eigenequation can be written similar to Eq.(1.5) as

$$H_{LF}\left|\psi\right\rangle = M^2\left|\psi\right\rangle. \tag{1.14}$$

For the many-body systems, the center of mass momentum is defined as follows,

$$\boldsymbol{P}_\perp = \sum_i \boldsymbol{p}_{i\perp}, \quad P^+ = \sum_i p_i^+. \tag{1.15}$$

It is convenient to introduce the longitudinal momentum fraction and the relative transverse momentum

$$x_i = \frac{p_i^+}{P^+}, \quad \boldsymbol{k}_{i\perp} = \boldsymbol{p}_{i\perp} - x_i \boldsymbol{P}_\perp. \tag{1.16}$$

Therefore,

$$\sum_i x_i = 1, \quad \sum_i \boldsymbol{k}_{i\perp} = \boldsymbol{0}. \tag{1.17}$$

The many-body invariant mass squared is given by

$$M^2 = P^+P^- - \boldsymbol{P}_\perp^2 = \sum_i \frac{\boldsymbol{k}_{i\perp}^2 + m_i^2}{x_i}, \tag{1.18}$$

which could be verified by using the sum of the on-energy shell p^- values to define the total P^- in

$$\begin{aligned} P^+P^- &= P^+ \sum_i \frac{(\boldsymbol{k}_{i\perp} + x_i \boldsymbol{P}_\perp)^2 + m^2}{x_i P^+} \\ &= \sum_i \frac{\boldsymbol{k}_{i\perp}^2 + 2x_i \boldsymbol{k}_{i\perp}\boldsymbol{P}_\perp + x_i^2 \boldsymbol{P}_\perp^2 + m_i^2}{x_i} \\ &= \sum_i \frac{\boldsymbol{k}_{i\perp}^2 + m_i^2}{x_i} + 2\sum_i \boldsymbol{k}_{i\perp}\boldsymbol{P}_\perp + \sum_i x_i \boldsymbol{P}_\perp^2 \\ &= \sum_i \frac{\boldsymbol{k}_{i\perp}^2 + m_i^2}{x_i} + \boldsymbol{P}_\perp^2, \end{aligned} \tag{1.19}$$

where the last equality follows Eq.(1.17). Note the momentum is not on the light-front energy shell.

CHAPTER 2. BLFQ MANY-BODY HAMILTONIAN

2.1 Two-body effective Hamiltonian

Heavy quarkonium is a bound-state system consisting primarily of the heavy quark-antiquark ($q\bar{q}$) pairs. The term "heavy quarkonium" usually refers to charmonium ($c\bar{c}$) and bottomonium ($b\bar{b}$), since the top quark is too heavy to form a long-lifetime bound state. There are plentiful experimental results for heavy quarkonia, so it has been a great testing ground for theories and models [4]. A quarkonium state $|\psi_h\rangle$ understood to be a superposition of various eigenstates in the Fock space, namely,

$$|\psi_h\rangle = c_1 |q\bar{q}\rangle + c_2 |q\bar{q}g\rangle + c_3 |q\bar{q}q\bar{q}\rangle + c_4 |q\bar{q}q\bar{q}g\rangle + \dots . \tag{2.1}$$

A full treatment of the quarkonium state is therefore complicated. However, heavy quarkonia are understood to be approximately in a non-relativistic bound state since the quark mass is much larger than the scale of non-perturbative physics. Thus different non-relativistic calculation schemes are often adopted: non-relativistic potential models [5], non-relativistic QCD [6], effective field theory [7], and etc. It is a reasonable conjecture that in the heavy quarkonium, the $|q\bar{q}\rangle$ sector dominates every other sectors in Eq.(2.1). To study heavy quarkonium, one can add the phenomenological correction terms such as confining potential and Coulomb-like potential to describe interactions. These treatments, with their parameters adjusted to fit experimental data, work successfully in describing the masses, decay width and other properties of the heavy quarkonium [8].

There is little difficulty to implement similar ideas to light front and, at the same time, develop a fully relativistic approach that could be useful for a wider range of systems. As we have obtained the invariant mass for two-body system, we could add a effective potential on the $|q\bar{q}\rangle$ sector to describe interactions

$$H = \frac{\boldsymbol{p}_\perp^2 + m_q^2}{x(1-x)} + V_{\text{eff}}, \tag{2.2}$$

where m_q is the constituent quark mass (taken to be the same as the antiquark mass), $x \equiv p_q^+/P^+$ and $(1-x)$ represent the longitudinal momentum fraction of the quark and antiquark respectively. The problem amounts to solving the eigenequation on the light front

$$H\,|\psi_h(\boldsymbol{p},x)\rangle = M_h^2\,|\psi_h(\boldsymbol{p},x)\rangle\,. \tag{2.3}$$

From a phenomenological point of view, we desire the effective potential to include all non-perturbative dynamics of the theory.

The light-front holography, which is first introduced by Brodsky and de Téramond [9], is fairly successful in solving the QCD bound-state problems. Among several options, the soft-wall model was originally designed for the light mesons. In this model, one drops the quark mass in the light-front kinetic energy term, while adding the transverse confinement. Specifically, the effective soft-wall (SW) Hamiltonian is given by

$$H_{\rm SW} = \frac{\boldsymbol{p}_\perp^2}{x} + \frac{\boldsymbol{p}_\perp^2}{1-x} + \kappa^4\boldsymbol{\zeta}_\perp^2, \tag{2.4}$$

where κ is the confining strength. This effective Hamiltonian is a 2-dimensional (2D) harmonic oscillator represented by holographic variables $\boldsymbol{\zeta}_\perp = \sqrt{x(1-x)}\boldsymbol{r}_\perp$, and its conjugate momenta $\boldsymbol{q}_\perp = \boldsymbol{p}_\perp/\sqrt{x(1-x)}$. Due to the 2D rotational symmetry, the Hamiltonian is degenerate, hence there are different choices of a complete basis to represent the eigenfunctions based on the specific strategy of Hamiltonian decomposition. In the soft-wall model, the particular eigenfunctions are chosen as

$$\phi_{\mathtt{nm}}(\boldsymbol{q}_\perp,b) = b^{-1}\sqrt{\frac{4\pi\mathtt{n}!}{(\mathtt{n}+|\mathtt{m}|)!}}\left(\frac{q_\perp}{b}\right)^{|\mathtt{m}|} e^{-q_\perp^2/b^2} L_{\mathtt{n}}^{|\mathtt{m}|}(q_\perp^2/b^2) e^{\mathrm{i}\mathtt{m}\theta}, \tag{2.5}$$

where $q_\perp = |\boldsymbol{q}_\perp|$, $\theta = \arg\boldsymbol{q}_\perp$, $\mathtt{n}$ and $\mathtt{m}$ are the radial quantum number and angular momentum projection, respectively. $L_{\mathtt{n}}^{\mathtt{m}}(x)$ is the associated Laguerre polynomial, and b is the energy scale of the harmonic oscillator. We usually set $b \equiv \kappa$ to match the confining strength according to Ref. [10] . Therefore the corresponding eigenvalues are

$$E_{\mathtt{nm}} = 2\kappa^2\big(2\mathtt{n}+|\mathtt{m}|+1\big), \tag{2.6}$$

with $\mathtt{n} = 0, 1, 2, ...$, and $\mathtt{m} = 0, \pm1, \pm2, ...$ This choice is useful when it comes to identifying meson states in BLFQ approach [10].

Inspired by the soft-wall model in light-front holography, Li has incorporated the model within BLFQ to study heavy quarkonium [10]. In heavy quarkonium, the quark mass can no longer be omitted. So we bring back the mass terms which was omitted in the soft-wall model. In addition, a longitudinal confinement potential is introduced, and therefore the longitudinal degree of freedom is now included. The Hamiltonian then reads

$$H_0 = \frac{\boldsymbol{p}_\perp^2 + m_q^2}{x} + \frac{\boldsymbol{p}_\perp^2 + m_{\bar{q}}^2}{1-x} + \kappa^4 \boldsymbol{\zeta}_\perp^2 + V_{\rm L}(x), \tag{2.7}$$

where m_q ($m_{\bar{q}}$) is the (anti-) quark mass, $V_{\rm L}$ is the confining potential in the longitudinal direction. Particularly, the longitudinal confinement is proposed in the following form,

$$V_{\rm L} = -\frac{\kappa^4}{(m_q + m_{\bar{q}})^2} \partial_x \big(x(1-x)\partial_x\big), \tag{2.8}$$

where $\partial_x \equiv (\partial/\partial x)|_{\boldsymbol{\zeta}_\perp}$. There are several advantages to present the longitudinal confinement in such a way,

- Introduces the longitudinal excitation mode with analytical eigenfunctions;
- In the massless limit, i.e., $m_q \ll \kappa$, the longitudinal excitations has very high energy, in which case the system tends to remain in the longitudinal ground state mode. Meanwhile the longitudinal ground state eigenfunction is a constant. Hence it recovers the soft-wall model;
- The obtained longitudinal eigenfunctions resemble the perturbative QCD asymptotic parton distributions;
- Reduces to z component of the 3-dimensional (3D) harmonic oscillator potential in the non-relativistic limit.

As the eigenfunction for transverse direction in Eq.(2.5), in the longitudinal direction, we have

$$\chi_{\mathtt{l}}(x;\alpha,\beta) = \sqrt{4\pi(2\mathtt{l}+\alpha+\beta+1)}\sqrt{\frac{\Gamma(\mathtt{l}+1)\Gamma(\mathtt{l}+\alpha+\beta+1)}{\Gamma(\mathtt{l}+\alpha+1)\Gamma(\mathtt{l}+\beta+1)}} x^{\frac{\beta}{2}}(1-x)^{\frac{\alpha}{2}} J_{\mathtt{l}}^{\alpha,\beta}(2x-1), \tag{2.9}$$

where $J_{\mathtt{l}}^{\alpha,\beta}(2x-1)$ is the Jacobi polynomial, $\alpha = 2m_{\bar{q}}(m_q + m_{\bar{q}})/\kappa^2$ and $\beta = 2m_q(m_q + m_{\bar{q}})/\kappa^2$ are dimensionless basis parameters in the model [10].

Now the Hamiltonian with longitudinal confinement potential becomes

$$H_0 = \frac{\boldsymbol{p}_\perp^2 + m_q^2}{x} + \frac{\boldsymbol{p}_\perp^2 + m_{\bar{q}}^2}{1-x} + \kappa^4 \boldsymbol{\zeta}_\perp^2 - \frac{\kappa^4}{(m_q + m_{\bar{q}})^2}\partial_x\big(x(1-x)\partial_x\big). \tag{2.10}$$

Note that H_0 is analytically solvable, with the eigenvalues being the mass squared of the bound states

$$M_{\mathtt{nml}}^2 = (m_q + m_{\bar{q}})^2 + 2\kappa^2(2\mathtt{n} + |\mathtt{m}| + \mathtt{l} + \frac{3}{2}) + \frac{\kappa^4}{(m_q + m_{\bar{q}})^2}\mathtt{l}(\mathtt{l}+1), \tag{2.11}$$

and the eigenfunctions

$$\Psi_{\mathtt{nml}}(\boldsymbol{p}_\perp, x) = \phi_{\mathtt{nm}}\Big(\boldsymbol{p}_\perp/\sqrt{x(1-x)}\Big)\chi_{\mathtt{l}}(x). \tag{2.12}$$

This Hamiltonian H_0 is often referred as the basis Hamiltonian, while $\Psi_{\mathtt{nml}}$ is known as the basis function.

The phenomenological Hamiltonian above provides a first approximation to heavy quarkonium, it mainly considers the long-distance physics, i.e., confinement. In addition to the given form of the basis Hamiltonian, an effective interaction which governs the short-range physics by one-gluon exchange V_g is also introduced [11]. Specifically,

$$V_g = -\frac{C_F 4\pi\alpha_s}{Q^2}\bar{u}_{s'}(k')\gamma_\mu u_s(k)\bar{v}_{\bar{s}}(\bar{k})\gamma^\mu v_{\bar{s}'}(\bar{k}'), \tag{2.13}$$

where $C_F = (N_c^2 - 1)/(2N_c) = 4/3$ is the color factor for the color singlet state, $Q^2 = -1/2(k' - k)^2 - 1/2(\bar{k}' - \bar{k})^2$ is the average 4-momentum squared transferred by the exchanged gluon. α_s is the coupling constant of QCD, which is set as either a constant or an effective running coupling in practical calculations [10, 12]. Note that this V_g term is introduced as an effective potential, so there is no dynamical gluon involved so far in this scenario, namely the Fock space is still restricted to $|q\bar{q}\rangle$, instead of extending to include $|q\bar{q}g\rangle$.

In total the overall effective Hamiltonian with confinement and effective interaction for the meson system reads

$$H_{\text{eff}} = \frac{\boldsymbol{p}_\perp^2 + m_q^2}{x} + \frac{\boldsymbol{p}_\perp^2 + m_{\bar{q}}^2}{1-x} + \kappa^4 \boldsymbol{\zeta}_\perp^2 - \frac{\kappa^4}{(m_q + m_{\bar{q}})^2}\partial_x\big(x(1-x)\partial_x\big) + V_g. \tag{2.14}$$

Now with the V_g term, the entire Hamiltonian matrix $H_{\rm eff}$ is no longer self-diagonal within the given basis. Instead, we solve the eigenvalue equation on the light front

$$H_{\rm eff}\,|\psi_h\rangle = M^2\,|\psi_h\rangle \tag{2.15}$$

for the bound state by diagonalizing the matrix numerically. By doing so, one obtains the eigenvalues which indicate the spectra as squared masses, and the light-front wave function (LFWF) expended on the eigenstates of the basis Hamiltonian H_0 as

$$\psi_{h/s\bar{s}}(\boldsymbol{p}_\perp, x) = \sum_{\mathtt{n},\mathtt{m},\mathtt{l}} \psi_h(\mathtt{n},\mathtt{m},\mathtt{l},s,\bar{s})\phi_{\mathtt{nm}}\Big(p_\perp/\sqrt{x(1-x)}\Big)\chi_{\mathtt{l}}(x). \tag{2.16}$$

The Hamiltonian $H_{\rm eff}$ has been studied and applied to heavy quarkonium. The spectroscopy is obtained and several hadronic observables are calculated through LFWFs, which provided reasonable agreement with experiment [10, 13, 14, 15]. In addition, it has also been extensively applied to other meson systems, such as the heavy-light [12], and light meson systems.

2.2 Jacobi transformation and its inverse

One significant feature of light-front dynamics is that, the intrinsic properties of bound state only depend on the relative motion of the constituents, which are characterized as the LFWFs. Therefore it is natural for us to work in the center of mass frame, in which the center of mass motion is omitted. Jacobi coordinates as well as momenta provide a proper set to work with because they separate the center of mass motion from the intrinsic motion. These Jacobi variables also provide a suitable set for defining all operators. The non-relativistic internal kinetic energy could be decoupled from the center of mass motion by proper choice of Jacobi coordinates. We shall see that in light-front dynamics, the kinetic energy can also be decoupled, and not surprisingly, the harmonic oscillator confining terms are also decoupled in such choice of coordinates. We use the term "Jacobi transformation" to refer the transformation from single particle coordinates and momenta to Jacobi coordinates and momenta. The variables defined in this section will be used throughout this thesis.

In the case of an n-body system, the space coordinate of each particle is labeled as $\boldsymbol{r}_i$. We assign the weight x_i, which is a variable defined to be positive, to the i-th particle for a certain physical property, for instance the longitudinal momentum fraction as in the previous section, that satisfies

$$\sum_{i=1}^{n} x_i = 1. \tag{2.17}$$

Let $X_k := \sum_{i=1}^{k} x_i$, then Eq.(2.17) is equivalent to $X_n = 1$.

Particularly, we define Jacobi coordinates and momenta as follows,

$$\begin{cases} \boldsymbol{\xi}_1 = \boldsymbol{r}_1 - \boldsymbol{r}_2 \\ \boldsymbol{\xi}_2 = \frac{1}{X_2}\left(x_1\boldsymbol{r}_1 + x_2\boldsymbol{r}_2\right) - \boldsymbol{r}_3 \\ \vdots \\ \boldsymbol{\xi}_i = \frac{1}{X_i}\sum_{k=1}^{i} x_k\boldsymbol{r}_k - \boldsymbol{r}_{i+1} \\ \vdots \\ \boldsymbol{\xi}_{n-1} = \frac{1}{X_{n-1}}\sum_{i=1}^{n-1} x_i\boldsymbol{r}_i - \boldsymbol{r}_n \\ \boldsymbol{R} := \boldsymbol{\xi}_n = \sum_{i=1}^{n} x_i\boldsymbol{r}_i \end{cases}, \quad \begin{cases} \boldsymbol{q}_1 = \frac{1}{X_2}\left(x_2\boldsymbol{p}_1 - x_1\boldsymbol{p}_2\right) \\ \boldsymbol{q}_2 = \frac{1}{X_3}\left(x_3\left(\boldsymbol{p}_1 + \boldsymbol{p}_2\right) - X_2\boldsymbol{p}_3\right) \\ \vdots \\ \boldsymbol{q}_i = \frac{1}{X_{i+1}}\left(x_{i+1}\sum_{k=1}^{i}\boldsymbol{p}_k - X_i\boldsymbol{p}_{i+1}\right) \\ \vdots \\ \boldsymbol{q}_{n-1} = \frac{1}{X_n}\left(x_n\sum_{i=1}^{n-1}\boldsymbol{p}_i - X_{n-1}\boldsymbol{p}_n\right) \\ \boldsymbol{P} := \boldsymbol{q}_n = \sum_{i=1}^{n}\boldsymbol{p}_i \end{cases}. \tag{2.18}$$

They could be understood in the following way: the j-th Jacobi coordinate ($j < n$) is the vector from the $j+1$-st particle to center of mass of the first j particles; j-th momentum can be regarded as total mass multiplies "relative velocity" between the subsystem formed by the first j particles and the $j+1$-st particle. Note that any permutation of particle assignment gives a different set of Jacobi coordinates when $n \geq 3$.

The Jacobi coordinates and momenta are canonical conjugate pairs

$$[\xi_i^a, q_j^b] = \mathrm{i}\delta_{ij}\delta_{ab}, \quad (i,j = 1,2,\ldots,n;\ a,b = 1,2,3) \tag{2.19}$$

where i, j are particle indices, and a, b are coordinate indices. This could be verified through a direct calculation: if both particle indices are smaller then n,

$$[\xi_i^a, q_j^b] = \begin{cases} \mathrm{i}\delta_{ab}\frac{x_{j+1}}{X_{j+1}}\left(\sum_{k=1}^{i}\frac{x_k}{X_i} - 1\right) = 0 & \text{if } i < j, \\ \mathrm{i}\delta_{ab}\left(\frac{x_{i+1}}{X_{i+1}}\sum_{k=1}^{i}\frac{x_k}{X_i} + \frac{X_i}{X_{i+1}}\right) = i\delta_{ab}\frac{x_{i+1}+X_i}{X_{i+1}} = i\delta_{ab} & \text{if } i = j, \\ \mathrm{i}\delta_{ab}\left(\frac{x_{j+1}}{X_{j+1}}\sum_{k=1}^{j}\frac{x_k}{X_i} - \frac{x_{j+1}}{X_i}\frac{X_j}{X_{j+1}}\right) = 0 & \text{if } i > j, \end{cases} \tag{2.20}$$

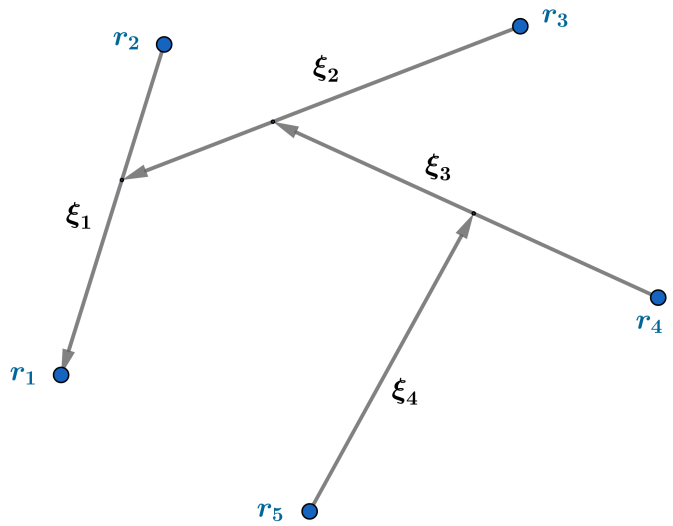

Figure 2.1 A possible set of Jacobi coordinates for five-body system. The labels on the blue dots signify the single particle coordinates while arrows presented are the Jacobi coordinates.

if at least one index equals to n,

$$[\xi_i^a, q_j^b] = \begin{cases} \mathrm{i}\delta_{ab}\left(\sum_{k=1}^{i}\frac{x_k}{X_i} - 1\right) = 0 & \text{if } i < n, j = n, \\ \mathrm{i}\delta_{ab}\left(\frac{x_{j+1}}{X_{j+1}}\sum_{k=1}^{j} x_k - \frac{x_{j+1}X_j}{X_{j+1}}\right) = 0 & \text{if } j < n, i = n, \\ \mathrm{i}\delta_{ab}\sum_{k+1}^{n} x_k = i\delta_{ab}. & \text{otherwise.} \end{cases} \tag{2.21}$$

The Jacobi transformation can be written as vector contraction $\boldsymbol{\xi} = R \cdot \boldsymbol{r}$, $\boldsymbol{q} = P \cdot \boldsymbol{p}$, where $\boldsymbol{v} = (\boldsymbol{v_1}, \cdots, \boldsymbol{v_n})$ for $\boldsymbol{v} = \boldsymbol{r}, \boldsymbol{\xi}, \boldsymbol{p}, \boldsymbol{q}$. The transformation matrix R and P are

$$R = \begin{pmatrix} 1 & -1 & & & \\ \frac{x_1}{X_2} & \frac{x_2}{X_2} & -1 & & \\ \vdots & \vdots & \ddots & \ddots & \\ \frac{x_1}{X_{n-1}} & \frac{x_2}{X_{n-1}} & \cdots & \frac{x_{n-1}}{X_{n-1}} & -1 \\ x_1 & x_2 & \cdots & x_{n-1} & x_n \end{pmatrix}, \quad P = \begin{pmatrix} \frac{x_2}{X_2} & \frac{-x_1}{X_2} & & & \\ \frac{x_3}{X_3} & \frac{x_3}{X_3} & \frac{-X_2}{X_3} & & \\ \vdots & \vdots & \ddots & \ddots & \\ \frac{x_n}{X_n} & \frac{x_n}{X_n} & \cdots & \frac{x_n}{X_n} & \frac{-X_{n-1}}{X_n} \\ 1 & 1 & \cdots & 1 & 1 \end{pmatrix}. \tag{2.22}$$

The following commutator calculated using the transformation matrices gives

$$\begin{aligned}[\xi_i^a, q_j^b] &= [R_{ik} r_k^a, P_{jl} p_l^b] = R_{ik} P_{jl} [r_k^a, p_l^b] \\ &= \mathrm{i}\delta_{ab}\delta_{kl} R_{ik} P_{jl} = \mathrm{i}\delta_{ab} R_{ik} P_{jk} = \mathrm{i}\delta_{ab} R P^{\mathsf{T}}{}_{ij},\end{aligned} \tag{2.23}$$

compare to the commutation relation (2.19),

$$R P^{\mathsf{T}}{}_{ij} = \delta_{ij}, \quad R P^{\mathsf{T}} = I_n = P R^{\mathsf{T}}, \tag{2.24}$$

one can obtain the inverse of Jacobi transformations

$$\boldsymbol{r} = P^{\mathsf{T}} \cdot \boldsymbol{\xi}, \quad \boldsymbol{p} = R^{\mathsf{T}} \cdot \boldsymbol{q}. \tag{2.25}$$

We will use the inverse Jacobi transformation to generalize the two-body Hamiltonian to many-body in the next section.

2.3 Generalization process

In general, the light-front effective Hamiltonian for the n-body system, treated as n-constituent particle systems, can be written as

$$H = \sum_i \frac{\boldsymbol{p}_{i\perp}^2 + m_i^2}{x_i} + \frac{1}{2!}\sum_{i,j} V_{ij}^{(2)} + \frac{1}{3!}\sum_{i,j,k} V_{ijk}^{(3)} + \dots. \tag{2.26}$$

The first term is the light-front kinetic energy with the conditions

$$\sum_i \boldsymbol{p}_{i\perp} = 0, \quad \sum_i x_i = 1, \tag{2.27}$$

because of momentum conservation. The interactions are written in terms of the cluster hierarchy of the interaction, starting from two-body. In this section we construct a basis Hamiltonian for a many-body system based on the two-body basis Hamiltonian in Eq.(2.7).

The kinetic energy operator in the n-body sector is

$$T = \sum_{i=1}^{n} \frac{\boldsymbol{p}_{i\perp}^2 + m_i^2}{x_i} - \boldsymbol{P}_\perp^2. \tag{2.28}$$

Note that the "pure mass" term $\sum_{i=1}^{n} m_i^2/x_i$ will be absorbed in the longitudinal confinement and the remaining part is called reduced kinetic energy

$$T_r = \sum_{i=1}^{n} \frac{\boldsymbol{p}_{i\perp}^2}{x_i} - \boldsymbol{P}_\perp^2. \tag{2.29}$$

From now on, we shall refer to "reduced kinetic energy" as "kinetic energy."

The kinetic energy can be written in terms of Jacobi variables as a diagonal quadratic quantity. Using inverse transformation $\boldsymbol{p} = R^\intercal \cdot \boldsymbol{q}$, the kinetic energy can be written as a vector contraction

$$\sum_{i=1}^{n} \frac{\boldsymbol{p}_{i\perp}^2}{x_i} = \boldsymbol{p}_a \cdot X^{-1} \cdot \boldsymbol{p}_a = \boldsymbol{q}_a \cdot RX^{-1}R^\intercal \cdot \boldsymbol{q}_a, \tag{2.30}$$

where $X = \mathrm{diag}(1/x_1, \ldots, 1/x_n)$, $v_a = (v_1^a, \cdots, v_n^a)$, $v = \boldsymbol{p}, \boldsymbol{q}$, $a = 1, 2$ are the transverse components. Note that the index a appears doubly thus is summed up. The following observations are helpful to calculate the matrix element of $RX^{-1}R^\intercal$: $\sum_j R_{ij} = 0$ if $i < n$ and $R_{ij}/x_j = 1/X_i$ if $j \le i$. As for the off-diagonals we may assume $l < m$ without loss of generality, then

$$RX^{-1}R^\intercal_{ml} = \sum_{i=1}^{n} \frac{1}{x_i} R_{li} R_{mi} = \frac{1}{X_m} \sum_{i=1}^{l+1} R_{li} = 0. \tag{2.31}$$

For the diagonals

$$RX^{-1}R^\intercal_{ll} = \sum_{i=1}^{n} \frac{1}{x_i} R_{li} R_{li} = \begin{cases} \frac{1}{x_{i+1}} + \frac{1}{X_i} = \frac{1}{\eta_i} & \text{if } l < n \\ \sum_{i=1}^{n} x_i = 1 & \text{if } l = n, \end{cases} \tag{2.32}$$

where $\eta_i = x_{i+1}X_i/X_{i+1}$ for $i = 1, \ldots, n-1$. We further define $\eta_n = 1$ and combine Eq.(2.31) with Eq.(2.32) to obtain

$$RX^{-1}R^\intercal = \mathrm{diag}(1/\eta_1, \ldots, 1/\eta_{n-1}, 1/\eta_n) = Y^{-1}, \tag{2.33}$$

where $Y = \mathrm{diag}(\eta_1, \ldots, \eta_{n-1}, \eta_n)$. Therefore the kinetic energy in terms of Jacobi momenta is

$$T_r = \sum_{i=1}^{n} \frac{\boldsymbol{p}_{i\perp}^2}{x_i} - \boldsymbol{P}_\perp^2 = \sum_{i=1}^{n-1} \frac{\boldsymbol{q}_{i\perp}^2}{\eta_i}. \tag{2.34}$$

In the transverse direction, we adopt the pairwise soft-wall confinement, which can be written in two equivalent forms,

$$V_{\mathrm{T}} = \kappa^4 \left(\sum_{i=1}^{n} x_i \boldsymbol{r}_{i\perp} - \boldsymbol{R}_\perp^2 \right) = \kappa^4 \sum_{i<j}^{n} x_i x_j (\boldsymbol{r}_{i\perp} - \boldsymbol{r}_{j\perp})^2, \tag{2.35}$$

which can also be represented quadratically by Jacobi coordinates. We write $V_{\rm T}$ as vector contraction

$$\sum_{i=1}^{n} x_i \boldsymbol{r}_{i\perp}^2 = \boldsymbol{r}_a \cdot X \cdot \boldsymbol{r}_a = \boldsymbol{\xi}_a \cdot PXP^{\intercal} \cdot \boldsymbol{\xi}_a. \tag{2.36}$$

From Eq.(2.33) we have

$$PXP^{\intercal} = (RX^{-1}R^{\intercal})^{-1} = Y, \tag{2.37}$$

therefore the potential can be written as

$$V_{\rm T} = \kappa^4 \left(\sum_{i=1}^{n} x_i \boldsymbol{r}_{i\perp}^2 - \boldsymbol{R}_{\perp}^2 \right) = \kappa^4 \sum_{i}^{n-1} \eta_i \boldsymbol{\xi}_{i\perp}^2. \tag{2.38}$$

Combining Eq.(2.34) and Eq.(2.38), the transverse Hamiltonian reads

$$H_{\rm T} = T_r + V_{\rm T} = \sum_{i=1}^{n-1} \left(\frac{\boldsymbol{q}_{i\perp}^2}{\eta_i} + \kappa^4 \eta_i \boldsymbol{\xi}_{i\perp}^2 \right), \tag{2.39}$$

which consists of $n-1$ independent 2D harmonic oscillators.

The generalization of the longitudinal confinement $V_{\rm L}$ requires more deliberation. In the two-body system,

$$V_{\rm L} = -\frac{\kappa^4}{(m_1+m_2)^2} \partial_x \left(x\left(1-x\right) \partial_x \right). \tag{2.40}$$

The following treatment is helpful to calculate the longitudinal confinement in the non-relativistic limit,

$$\partial_x \equiv \frac{\partial}{\partial x} = \frac{\partial}{\partial q_{1z}} \frac{\partial q_{1z}}{\partial x} = (m_1+m_2) \frac{\partial}{\partial q_{1z}} = \mathrm{i}(m_1+m_2)(r_{1z}-r_{2z}), \tag{2.41}$$

since the conjugate coordinate of q_{1z} is $(r_{1z}-r_{2z})$. If we keep everything in the leading order, the confinement can be written as

$$V_{\rm L} = -\frac{\kappa^4}{(m_1+m_2)^2} \partial_x \left(x\left(1-x\right) \partial_x \right) = \frac{m_1 m_2 \kappa^4}{(m_1+m_2)^2} (r_{1z}-r_{2z})^2 \approx x_1 x_2 (r_{1z}-r_{2z})^2, \tag{2.42}$$

which agrees with the harmonic oscillator potential we expected in the z direction. Together with the transverse potential $V_T = x_1 x_2 (r_{1\perp}-r_{2\perp})^2$, we have recovered the full harmonic oscillator potential in coordinate space.

Unfortunately, this can not be generalized to a system of n particle if $n > 2$ in a straightforward way: Naively, let $\gamma_{ab} = x_a/(x_a + x_b)$ be the relative longitudinal momentum fraction of the pair of particles a and b, the generalized longitudinal confinement could be

$$V_{\rm L} = -\frac{1}{2}\kappa^4 \sum_{a\neq b} \frac{1}{(m_a + m_b)^2} \partial_{\gamma_{ab}} \left(\gamma_{ab}\,(1-\gamma_{ab})\,\partial_{\gamma_{ab}}\right). \tag{2.43}$$

But actually it is not well defined. The possible number of pairs of particles is $n(n-1)/2$ which is greater than the degrees of freedom $n-1$ if $n > 2$.

We now proposed a general formalism of longitudinal confinement for many-body system which can be reduced to harmonic oscillator in z direction. Suppose we have an n-body system, in addition to the variables related to Jacobi coordinates defined in Chap.(2.2), we define the partial total constituent mass $M_i = \sum_{k=1}^{i} m_i$, partial total momentum (in z direction) $P_{z,i} = \sum_{k=1}^{i} p_{z,k}$, and partial momentum fraction $\gamma_i = x_{i+1}/X_{i+1}, (i = 1, \ldots, n-1)$. The proposed potential is

$$V = -\sum_{i=1}^{n-1} \frac{1}{X_{i+1}} \partial_{\gamma_i} \left(\gamma_i\,(1-\gamma_i)\,\partial_{\gamma_i}\right). \tag{2.44}$$

When $n = 2$, the potentials are the corresponding longitudinal confinement in our two-body model off by a factor κ^4/M^2 where M is the total constituent mass. We will see later in this section that the coefficient κ^4/M^2 is not a coincidence. Note that we employee X_i in Eq.(2.44) for convenience, the real set of free parameters should be γ_i.

To verify this confinement reduces to harmonic oscillator potential in the non-relativistic limit in z direction, we first calculate γ_i in the leading order,

$$\gamma_i = \frac{x_{i+1}}{X_{i+1}} = \frac{e_{i+1} + p_{z,i+1}}{\sum_{k=1}^{i+1}(e_{k+1} + p_{z,k+1})} = \frac{m_{i+1} + p_{z,i+1}}{M_{i+1} + P_{z,i+1}} + o(p^2), \tag{2.45}$$

where the term $o(p^2)$ is due to $e_i = \sqrt{m_i^2 + p_i^2} = m_i + o(p_i^2)$. We then drop the higher order term and expand Eq.(2.45) to the leading order

$$\begin{aligned} \frac{m_{i+1} + p_{z,i+1}}{M_{i+1} + P_{z,i+1}} &= \frac{1}{M_{i+1}^2}(M_{i+1}m_{i+1} + p_{z,i+1}M_{i+1} + P_{z,i+1}m_{i+1}) + o(p_z) \\ &= \frac{1}{M_{i+1}}(m_{i+1} + q_{z,i}) + o(p_z), \end{aligned} \tag{2.46}$$

where $q_{z,i}$ is the i-th Jacobi momentum in z direction. Hence we have the relation

$$\partial_{\gamma_i} = M_{i+1}\partial_{q_i} = \mathrm{i}M_{i+1}\xi_i \tag{2.47}$$

where ξ_i is the i-th Jacobi coordinate in z direction. Note that in the leading order, $x_i = m_i/M$, $X_i = M_i/M$, $\gamma_i = m_{i+1}/M_{i+1}$. The potential becomes

$$\begin{aligned} V &= -\sum_{i=1}^{n-1} \frac{1}{X_{i+1}} \partial_{\gamma_i} \left(\gamma_i \left(1-\gamma_i\right) \partial_{\gamma_i}\right) = -\sum_{i=1}^{n-1} \frac{1}{X_{i+1}} (\mathrm{i}M_{i+1}\xi_i)^2 \cdot \frac{m_{i+1}M_i}{M_{i+1}^2} \\ &= M^2 \sum_{i=1}^{n-1} \frac{m_{i+1}M_i}{MM_{i+1}} \xi_i^2 = M^2 \sum_{i=1}^{n-1} \eta_i \xi_i^2 = M^2 \sum_{i<j}^{n} x_i x_j (r_{z,i} - r_{z,j})^2. \end{aligned} \tag{2.48}$$

Multiply V by a factor κ^4/M^2 gives the harmonic oscillator in z direction.

Finally, the basis Hamiltonian combining both transverse and longitudinal directions is

$$H_0 = \sum_{i=1}^{n-1} \left(\frac{\boldsymbol{q}_{i\perp}^2}{\eta_i} + \kappa^4 \eta_i \boldsymbol{\xi}_{i\perp}^2\right) - \frac{\kappa^4}{M^2} \sum_{i=1}^{n-1} \frac{1}{X_{i+1}} \partial_{\gamma_i} \left(\gamma_i \left(1-\gamma_i\right) \partial_{\gamma_i}\right) + \sum_{i=1}^{n} \frac{m_i}{x_i}. \tag{2.49}$$

and we call $H_{\mathrm{L}} = H_0 - H_{\mathrm{T}}$ the longitudinal Hamiltonian. The eigenfunctions are analytically known, we will study the case when $n = 3$ in detail in the next section to gain some insights. Moreover, our generalization has the capability of assigning particles to different clusters depending on the physical system we are interested in. Details can be found in Appendix A.

2.4 Three-body effective Hamiltonian

As suggested in the preceding arguments, the desired three-body Hamiltonian is

$$\begin{aligned} H_{\mathrm{eff}} &= \sum_{i=1}^{2} \left(\frac{\boldsymbol{q}_{i\perp}^2}{\eta_i} + \kappa^4 \eta_i \boldsymbol{\xi}_{i\perp}^2\right) - \frac{\kappa^4}{M^2} \sum_{i=1}^{2} \frac{1}{X_{i+1}} \partial_{\gamma_i} \left(\gamma_i \left(1-\gamma_i\right) \partial_{\gamma_i}\right) + \sum_{i=1}^{2} \frac{m_i}{x_i} + V_g \\ &= H_{\mathrm{T}} + H_{\mathrm{L}} + V_g, \end{aligned} \tag{2.50}$$

where H_{T} and H_{L} are transverse and longitudinal Hamiltonian respectively and V_g is the one-gluon exchange. At the present stage, we do not include the one-gluon exchange term, but instead, we use a constant to compensate the lack of short distance physics which serves as a correction to the eigenvalues. Note that the constant term will only shift the eigenvalues but not introduce changes to eigenfunctions. We drop the constant term for the rest of this section. The basis

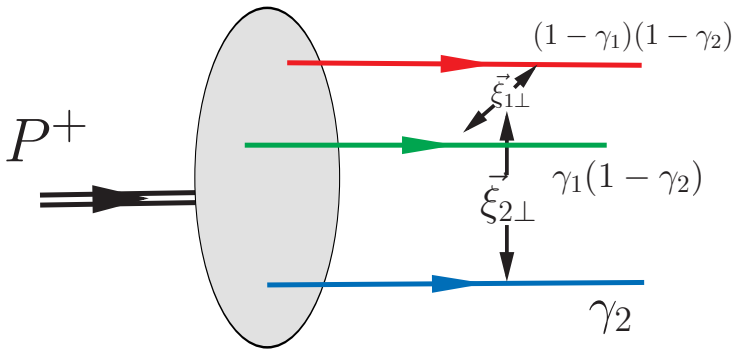

Figure 2.2 Visualization of three-body Jacobi coordinates and longitudinal momentum fraction represented by relative longitudinal momentum fraction $\gamma_i = x_{i+1}/X_{i+1}$.

Hamiltonian $H_0 = H_{\rm T} + H_{\rm L}$ is separable to transverse and longitudinal directions, therefore finding the eigenfunction of H_0 is equivalent to finding eigenfunctions of $H_{\rm T}$ and $H_{\rm L}$.

Explicitly, the Jacobi variables for the three-body system reads

$$\begin{aligned} \boldsymbol{q}_{1\perp} &= \frac{x_1\boldsymbol{p}_{2\perp} - x_2\boldsymbol{p}_{1\perp}}{x_1+x_2}, \quad \boldsymbol{\xi}_{1\perp} = \boldsymbol{r}_{2\perp} - \boldsymbol{r}_{1\perp}, \quad \eta_1 = \frac{x_1x_2}{x_1+x_2}, \\ \boldsymbol{q}_{2\perp} &= \boldsymbol{p}_{3\perp} - x_3\boldsymbol{P}_\perp, \quad \boldsymbol{\xi}_{2\perp} = \frac{\boldsymbol{r}_{3\perp} - \boldsymbol{R}_\perp}{1-x_3}, \quad \eta_2 = x_3(x_1+x_2). \end{aligned} \tag{2.51}$$

We define the generalized holographic variables

$$\boldsymbol{\tau}_{i\perp} \equiv \frac{\boldsymbol{q}_{i\perp}}{\sqrt{\eta_i}}, \quad \boldsymbol{\zeta}_{i\perp} \equiv \sqrt{\eta_i}\boldsymbol{\xi}_{i\perp}, \quad (i=1,2). \tag{2.52}$$

The transverse Hamiltonian reads

$$H_{\rm T} = \boldsymbol{\tau}_{1\perp}^2 + \kappa^4\boldsymbol{\zeta}_{1\perp}^2 + \boldsymbol{\tau}_{2\perp}^2 + \kappa^4\boldsymbol{\zeta}_{2\perp}^2, \tag{2.53}$$

which clearly consists of two 2D harmonic oscillators since τ_i, and ζ_i $(i=1,2)$ are canonical conjugate pairs. The eigenvalues are the sum of eigenvalues of two 2D harmonic oscillators

$$E_{\rm T} = 2\kappa^2(2\mathtt{n}_1 + |\mathtt{m}_1| + 2\mathtt{n}_2 + |\mathtt{m}_2| + 2), \tag{2.54}$$

and the eigenfunctions in momentum space due to Eq.(2.5) can be written as $\phi_{\mathtt{n}_1\mathtt{m}_1}(\boldsymbol{\tau}_{1\perp})\phi_{\mathtt{n}_2\mathtt{m}_2}(\boldsymbol{\tau}_{2\perp})$.

To address the longitudinal Hamiltonian

$$\begin{aligned} H_{\rm L} =& \frac{m_3}{\gamma_2} + \frac{1}{1-\gamma_2}\left(\frac{m_2}{\gamma_1} + \frac{m_1}{1-\gamma_1}\right) \\ & - \frac{\kappa^4}{(m_1+m_2+m_3)^2}\left[\partial_{\gamma_2}(\gamma_2(1-\gamma_2)\partial_{\gamma_2}) + \frac{1}{1-\gamma_2}\partial_{\gamma_1}(\gamma_1(1-\gamma_1)\partial_{\gamma_1})\right], \end{aligned} \tag{2.55}$$

we express the mass term in the kinetic energy as

$$\frac{m_1}{x_1}+\frac{m_2}{x_2}+\frac{m_3}{x_3}=\frac{m_3}{\gamma_2}+\frac{1}{1-\gamma_2}\left(\frac{m_2}{\gamma_1}+\frac{m_1}{1-\gamma_1}\right), \tag{2.56}$$

where $\gamma_i = x_{i+1}/X_{i+1}$ are the relative longitudinal momentum transfer. We then rewrite $H_{\rm L}$ as

$$H_{\rm L}=\frac{m_3^2}{\gamma_2}+\frac{\mathcal{M}^2}{1-\gamma_2}-\frac{\kappa^4}{(m_1+m_2+m_3)^2}\partial_{\gamma_2}\big(\gamma_2(1-\gamma_2)\partial_{\gamma_2}\big), \tag{2.57}$$

where $\mathcal{M}^2$ is an operator

$$\mathcal{M}^2=\frac{m_2^2}{\gamma_1}+\frac{m_1^2}{1-\gamma_1}-\frac{\kappa^4}{(m_1+m_2+m_3)^2}\partial_{\gamma_1}\big(\gamma_1(1-\gamma_1)\partial_{\gamma_1}\big). \tag{2.58}$$

Here $\mathcal{M}^2$ shares the same form as the longitudinal confinement in the two-body model from which the solution of equation $\mathcal{M}^2\chi_\ell(\gamma_1)=M_{\mathtt{l}_1}^2\chi_\ell(\gamma_1)$ can be obtained from Eq.(2.9) as

$$\chi_{\mathtt{l}_1}^{(A,B)}(\gamma_1)\equiv N\gamma_1^{B/2}\,(1-\gamma_1)^{A/2}\,J_{\mathtt{l}_1}^{A,B}\,(2\gamma_1-1)\,, \tag{2.59}$$

where N is the normalization constant, $A=2m_1(m_1+m_2+m_3)/\kappa^2$, $B=2m_2(m_1+m_2+m_3)/\kappa^2$, $M_{\mathtt{l}_1}$ is the eigenvalues satisfy

$$M_{\mathtt{l}_1}^2=(m_1+m_2)^2+\frac{m_1+m_2}{m_1+m_2+m_3}\kappa^2(2\mathtt{l}_1+1)+\frac{\kappa^4}{(m_1+m_2+m_3)^2}\mathtt{l}_1(\mathtt{l}_1+1). \tag{2.60}$$

Now consider a function of the form $\chi_{\mathtt{l}_1}^{(A,B)}(\gamma_1)f(\gamma_2)$, on which we act by $H_{\rm L}$,

$$\begin{aligned}H_{\rm L}f(\gamma_2)\chi_{\mathtt{l}_1}^{(A,B)}(\gamma_1)&=\left(\frac{m_3^2}{\gamma_2}+\frac{\mathcal{M}^2}{1-\gamma_2}-\frac{\kappa^4}{(m_1+m_2+m_3)^2}\partial_{\gamma_2}\big(\gamma_2(1-\gamma_2)\partial_{\gamma_2}\big)\right)\chi_{\mathtt{l}_1}^{(A,B)}(\gamma_1)f(\gamma_2)\\&=\left(\frac{m_3^2}{\gamma_2}+\frac{M_{\mathtt{l}_1}^2}{1-\gamma_2}-\frac{\kappa^4}{(m_1+m_2+m_3)^2}\partial_{\gamma_2}\big(\gamma_2(1-\gamma_2)\partial_{\gamma_2}\big)\right)f(\gamma_2)\chi_{\mathtt{l}_1}^{(A,B)}(\gamma_1).\end{aligned} \tag{2.61}$$

If we take $f(\gamma_2)$ as $\chi_{\mathtt{l}_2}^{(\alpha_{\mathtt{l}1},\beta)}(\gamma_2)$, where $\alpha_{\mathtt{l}1}=2M_{\mathtt{l}1}(m_1+m_2+m_3)/\kappa^2$, $\beta=2m_3(m_1+m_2+m_3)/\kappa^2$, we construct the eigenfunction of the overall effective Hamiltonian $H_{\rm eff}$. One can see the derivation steps are of a recursion fashion.

Putting everything together, we obtain the the eigenfunctions of $H_{\rm eff}$

$$\Phi_{\mathtt{n}_1\mathtt{m}_1\mathtt{n}_2\mathtt{m}_2\mathtt{l}_1\mathtt{l}_2}(\boldsymbol{\tau}_{1\perp},\gamma_2,\boldsymbol{\tau}_{2\perp},\gamma_1)=\phi_{\mathtt{n}_1\mathtt{m}_1}(\boldsymbol{\tau}_{1\perp})\chi_{\mathtt{l}1}^{(A,B)}(\gamma_1)\phi_{\mathtt{n}_2\mathtt{m}_2}(\boldsymbol{\tau}_{2\perp})\chi_{\mathtt{l}2}^{(\alpha_{\mathtt{l}1},\beta)}(\gamma_2). \tag{2.62}$$

where $A = 2m_1(m_1+m_2+m_3)/\kappa^2$, $B = 2m_2(m_1+m_2+m_3)/\kappa^2$, and $\alpha_{11} = 2M_{11}(m_1+m_2+m_3)/\kappa^2$, $\beta = 2m_3(m_1+m_2+m_3)/\kappa^2$. With corresponding mass eigenvalues

$$E_{\mathtt{n}_1,\mathtt{m}_1,\mathtt{n}_2,\mathtt{m}_2,\mathtt{l}_1,\mathtt{l}_2} = (m_3+M_{\mathtt{l}_1})^2 + 2\kappa^2(2\mathtt{n}_1+|\mathtt{m}_1|+2\mathtt{n}_2+|\mathtt{m}_2|+2) + \frac{M_{\mathtt{l}_1}+m_3}{m_1+m_2+m_3}\kappa^2(2\mathtt{l}_2+1) + \frac{\kappa^4}{(m_1+m_2+m_3)^2}\mathtt{l}_2(\mathtt{l}_2+1). \quad (2.63)$$

In the next chapter, we will apply this model to nucleons.

CHAPTER 3. RESULTS AND OUTLOOK

3.1 Mass spectrum

We now investigate the nucleon mass spectrum with the BLFQ approach. In this work, we do not distinguish the up (u) and down (d) quarks in terms of their masses nor their other distinguishing features. That is, in the spirit of the AdS/QCD approach, we solve the model introduced here neglecting spin, color and Pauli statistics. Reflected in the model, that is $m_1 = m_2 = m_3 = m$. Therefore, the ground state mass squared of the nucleon is given by

$$M_0^2 = \left(m + \sqrt{4m^2 + \frac{2\kappa^2}{3}} \right)^2 + 5\kappa^2 + \left(\sqrt{\frac{4}{9} + \frac{2\kappa^2}{27m^2}} - \frac{2}{3} \right) \kappa^2 + \text{Const}, \tag{3.1}$$

where κ is the confining strength of the bound state, demonstrating the interaction between particle pairs. As $\kappa \to 0$, there is no mass splitting among the states, in which case the nucleon mass becomes the sum of the three constituent quark masses. We take m, κ and the constant as adjustable parameters for the purpose of fitting the nucleon spectra.

A mass spectrum is shown in Fig. 3.1, where we compared our BLFQ result with AdS/QCD [9] and the experimental values collected by Particle Data Group (PDG) [16]. We select the states which have the parity $\mathsf{P} = +1$, spin $\mathsf{S} = 1/2$, and isospin $\mathsf{I} = 1/2$.

In this work, we start with the Hamiltonian without one-gluon exchange interaction. We choose the states which have even $\mathtt{l}_1 + \mathtt{l}_2 + N$ to preserve parity in the functional form, where $N \equiv 2\mathtt{n}_1 + |\mathtt{m}_1| + 2\mathtt{n}_2 + |\mathtt{m}_2|$ is the total excitation in transverse direction. We adopt $\kappa = 0.49$ GeV as the confining strength from Ref. [9], and also use $m = 0.35$ GeV which is obtained from fitting the elastic form factor (see details in chapter 3.2); finally we adjust the mass shift (the Const. term in Eq. (3.1)) to match the mass of the ground states, i.e. the proton. As a result of bringing in the longitudinal degree of freedom in BLFQ, we have more states than AdS/QCD. So in Table. 3.1 we only pick those states which are comparable with experiment data obtained from PDG. We expect

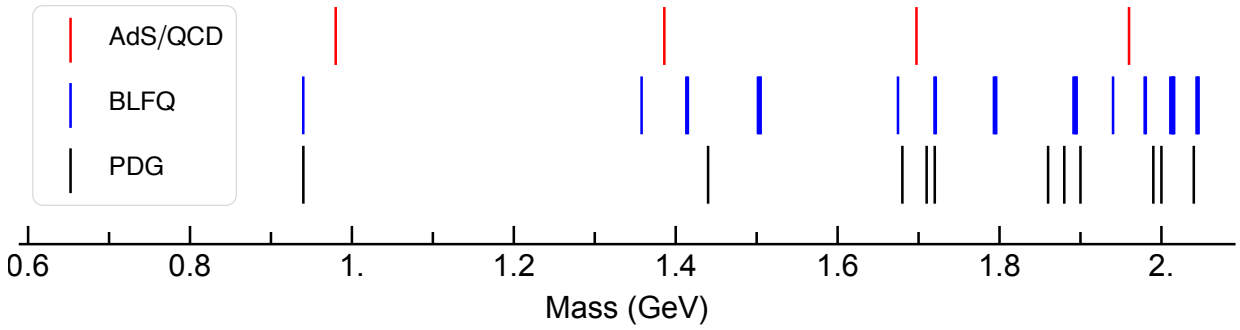

Figure 3.1 Representative spectrum of nucleons. We compare the result of this work (BLFQ) with Ads/QCD [9] and PDG [16]. The details of parameters we used for the spectrum are explained in the text.

Table 3.1 Selected mass eigenstates of BLFQ comparable to PDG. All masses are in GeV.

S	P	I	PDG	BLFQ
1/2	+	1/2	0.94	0.94
1/2	+	1/2	1.44	1.41
1/2	+	1/2	1.68	1.67
1/2	+	1/2	1.71	1.72
1/2	+	1/2	1.72	1.72
1/2	+	1/2	1.86	1.89
1/2	+	1/2	1.88	1.89
1/2	+	1/2	1.90	1.90
1/2	+	1/2	1.99	1.98
1/2	+	1/2	2.00	2.01
1/2	+	1/2	2.40	2.36

that the state density we obtain in the current simplified model to be higher than the experimental state density. Including the spin and spin-dependent one-gluon exchange interaction should lead to spreading of our spectrum in this low-mass region and reproduce more reasonable states density comparing with experiments. Also note that AdS/QCD has degeneracy starting from the first excitation mode due to rotation symmetry in SW model, which can be seen form Fig. 3.2 where the first excitation mode is the left end of the central yellow line.

In Fig. 3.2 we reproduce the Regge trajectory generated by AdS/QCD [9], at the same time we select some representative states comparable with those trajectories. The selecting scheme is the same as for Fig. 3.1.

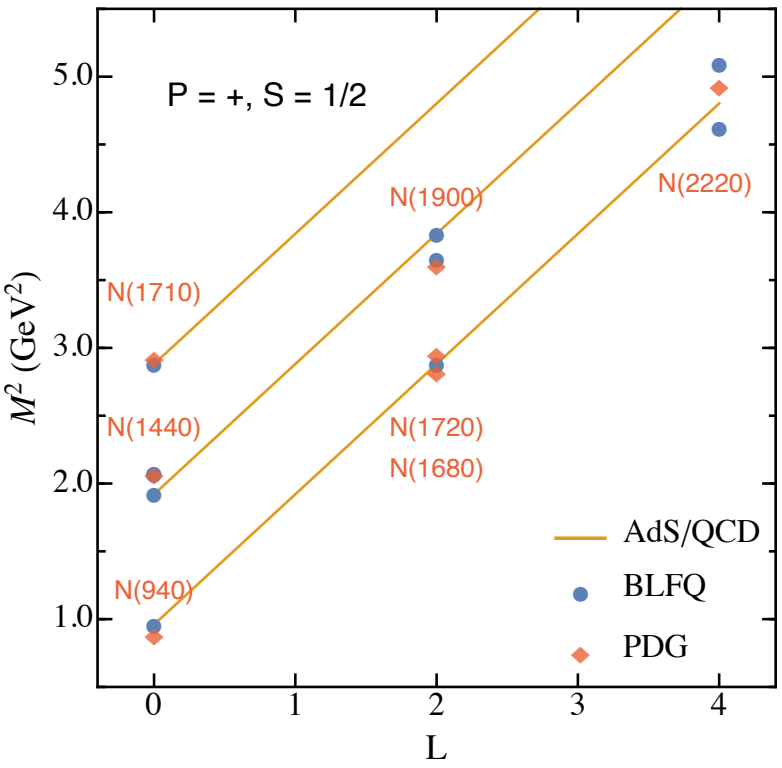

Figure 3.2 Regge trajectory of positive parity spin-half nucleons. The states obtained by AdS/QCD lies on the lines presented in the graph. Positive parity restricted the orbital angular momentum L to even number.

We emphasize that due to the lack of spin structure in the current model, we are unable to produce the states with other spin quantum numbers. There will be more useful results once we incorporate one-gluon exchange which is known to be important for spin splitting.

3.2 Elastic form factor at the ground state

The LFWFs provide us the direct access to hadron structures in the light-front framework. One can compute the experimental observables by simply integrating over the LFWFs with the relevant operators. Among several observables, the elastic form factor is a fundamental and significant quantity of great interest. Considering the feature of electric charge, we associate our system with the proton.

We first study the hadron matrix element of the current operator $J^\mu = \overline{\psi}\gamma^\mu\psi$ at $x^\mu = 0$. It relates to the electromagnetic form factors $F_1(q^2)$ and $F_2(q^2)$, also known as Dirac and Pauli form factor, respectively,

$$\big\langle\psi_h(P',\lambda')\big|J^\mu(0)\big|\psi_h(P,\lambda)\big\rangle = \bar{u}_{\lambda'}(\boldsymbol{p'})\Big[F_1(q^2)\gamma^\mu + F_2(q^2)\frac{\mathrm{i}}{2M}\sigma^{\mu\alpha}q_\alpha\Big]u_\lambda(\boldsymbol{p}), \tag{3.2}$$

where $q^\mu \equiv P'^\mu - P^\mu$ is the 4-momentum transfer, and $q^2 = q^\mu q_\mu$, λ (λ') refers to the helicity of the initial (final) state hadron, and M stands for the mass of hadron. For the sake of convenience, we adopt the "good current", i.e. $\mu = +$, and derive the relation within the Drell-Yan frame, where $q^+ = 0$ [17]. This indicates the probe photon is carrying 4-momentum $q^\mu \equiv (q^+, q^-, \boldsymbol{q}_\perp) = (0, -q^2/p^+, \boldsymbol{q}_\perp)$ along the transverse direction. Then the electromagnetic form factors can be written as

$$\begin{aligned}\big\langle\psi_h(P',\lambda)\big|\frac{J^+(0)}{2P^+}\big|\psi_h(P,\lambda)\big\rangle &= F_1(q^2),\\ \big\langle\psi_h(P',\uparrow)\big|\frac{J^+(0)}{2P^+}\big|\psi_h(P,\downarrow)\big\rangle &= -(q_1 - \mathrm{i}q_2)\frac{F_2(q^2)}{2M}.\end{aligned} \tag{3.3}$$

These show that $F_1(q^2)$ and $F_2(q^2)$ correspond to the helicity-conserving and helicity-flip matrix element of J^+, respectively. Due to the neglect of the one-gluon exchange, there is no information about the spin structure included in the current form of our Hamiltonian. We presume the helicity is conserved for the initial and final hadron states by applying the existing wave function. Therefore, the Dirac form factor $F_1(q^2)$ in the light-front wave function representation is given by [18, 19]

$$F_1(q^2) = \sum_n \sum_j e_j \int \prod_i \mathrm{d}x_i\ \mathrm{d}^2\boldsymbol{p}_{i\perp}\ \delta\left(1 - \sum_i x_i\right)\delta\left(\sum_i \boldsymbol{p}_{i\perp}\right)\left\{\psi_n^{\lambda *}(x_i, \boldsymbol{p}'_{i\perp})\psi_n^\lambda(x_i, \boldsymbol{p}_{i\perp})\right\}, \tag{3.4}$$

where ψ_n^λ is the n-body Fock-state wave function with helicity λ, e_j is the fractional charge of the struck constituent, and $\boldsymbol{p}'_{i\perp}$ is

$$\boldsymbol{p}'_{i\perp} = \begin{cases} \boldsymbol{p}'_{i\perp} - x_i \boldsymbol{q}_\perp & \text{if } i \neq j, \\ \boldsymbol{p}'_{i\perp} - (1-x_i)\boldsymbol{q}_\perp & \text{otherwise.} \end{cases} \tag{3.5}$$

This equation can be understood as the non-flip helicity wave function overlap and it is easily seen that $F_1(0) = 1$.

In our model, we treat our wave function as spin-independent. By doing this, we eliminate the helicity part of the wave function. We present our results for the Dirac form factor $F_1(q^2)$ at the ground state in Figs. 3.3-3.4 and compare with various experiments [20, 21, 22, 23, 24]. Details can be found in Appendix C. Since we carry out the calculation in the Drell-Yan frame and it produces the form factor in the space-like region ($q^2 < 0$), we employ $Q^2 = -q^2$ to illustrate the form factor. We associate it with the proton F_1, in which we set the parameters to be $\kappa = 0.49$ GeV, $m = 0.35$ GeV. $\kappa = 0.49$ GeV is adopted from Ref. [10]. We use data from different experiments to do comparisons.

The fitting in Fig. 3.4 shows deviation from experimental data in the larger Q^2 region. As a preliminary result without one-gluon exchange, one might naively expect the BLFQ to be lower than the experiments because by adding one-gluon exchange the wave functions will be flattened, which will would then cause the overlap to increase in the higher Q^2 region. We are optimistic that this issue will be resolved by introducing one-gluon exchange since we would then adjust the quark mass and the confinement interaction to obtain an overall fit to the charge form factor.

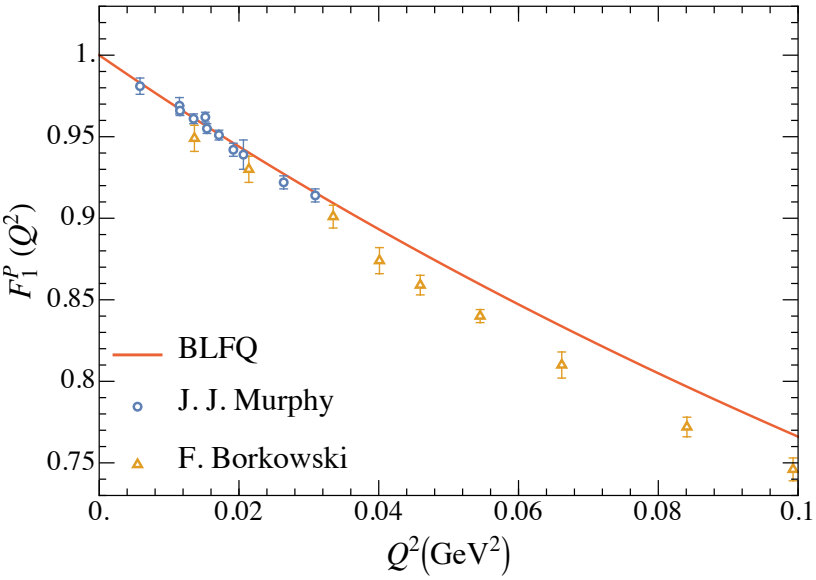

Figure 3.3 $F_1(Q^2)$ in the region 0 GeV^2-0.1 GeV^2 compared with experimental data with error bars for experimental uncertainties [20, 21].

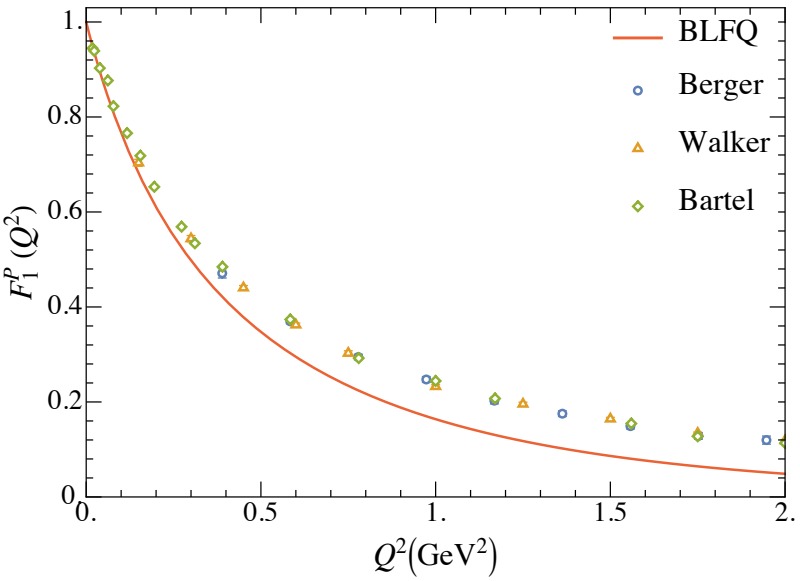

Figure 3.4 $F_1(Q^2)$ in the region 0 GeV^2-2 GeV^2 compared with a number of different experiment data with error bars showing experimental uncertainties [22, 23, 24].

3.3 One-gluon exchange

A natural improvement to this three-constituent quark model is to account for the effects of neglecting the $|qqqg\rangle$ Fock space. To do this we would develop an effective interaction, similar to the one-gluon exchange in mesons, but extended for baryons. Formally, it consists of gluon exchanges between 3 particle pairs,

$$V_g = V_{g12} + V_{g23} + V_{g31}, \tag{3.6}$$

where V_{gij} is the one-gluon exchange potential between particle i and j. Table 3.2 shows an example of the one-gluon exchange matrix, in which the matrix elements are calculated for the case that the exchange occurs between particle 1 and 2. For an observable baryon, the color state is singlet, in which case the a color factor of $-4/3$ should be applied. Note the results of different pairs are different due to the fact that assignment order in Jacobi transformation matters even though, they all can be calculated in a similar manner.

Table 3.2 The spinor part $\bar{u}_{s_1'}(p_1')\gamma_\mu u_{s_1}(p_1)\bar{u}_{s_2'}(p_2')\gamma^\mu u_{s_2}(p_2)$ in terms of three-body holographic variables, an overall factor $\delta_{s_3 s_{3'}}\delta(\sqrt{x(1-x)}k_2-\sqrt{x'(1-x')}k_{2'})$ should be applied if one wants to do integration due to momentum conservation.

	s_1	s_2	s_1'	s_2'	$\frac{1}{2}\bar{u}_{s_1'}(p_1')\gamma_\mu u_{s_1}(p_1)\bar{u}_{s_2'}(p_2')\gamma^\mu u_{s_2}(p_2) * \sqrt{\xi(1-\xi)\xi'(1-\xi')}(1-x)(1-x')$
①	+	+	+	+	$m_1^2(1-\xi)(1-x)(1-\xi')(1-x')+m_2^2\xi(1-x)\xi'(1-x')+$ $p_{2'}^* x_1' p_2 x_1 - p_{2'}^* x_1' p_1 x_2 + p_{1'}^* x_2' p_1 x_2 - p_{1'}^* x_2' p_1 x_2$
②	−	−	−	−	$m_1^2(1-\xi)(1-x)(1-\xi')(1-x')+m_2^2\xi(1-x)\xi'(1-x')+$ $p_{2'} x_1' p_2^* x_1 - p_{2'} x_1' p_1^* x_2 + p_{1'} x_2' p_1^* x_2 - p_{1'} x_2' p_1^* x_2$
③	+	−	+	−	$m_1^2(1-\xi)(1-x)(1-\xi')(1-x')+m_2^2\xi(1-x)\xi'(1-x')+$ $p_{2'} x_1' p_2^* x_1 + p_{1'}^* x_2' p_1 x_2 - p_{1'}^* x_2 p_{2'} x_1 - p_2^* x_2' p_1 x_1'$
④	−	+	−	+	$m_1^2(1-\xi)(1-x)(1-\xi')(1-x')+m_2^2\xi(1-x)\xi'(1-x')+$ $p_{2'} x_1' p_2^* x_1 + p_{1'}^* x_2' p_1 x_2 - p_{1'} x_2 p_{2'}^* x_1 - p_2 x_2' p_1^* x_1'$
⑤	+	+	+	−	$m_2\xi'(1-x')\big((\xi'\sqrt{x'(1-x')}k_{2'}^* + \sqrt{\xi'(1-\xi')}k_{1'}^*)(1-x'-(1-\xi)(1-x))-$ $(\xi\sqrt{x(1-x)}k_2^* + \sqrt{\xi(1-\xi)}k_1^*)(\xi'(1-x'))\big)$
⑥	−	−	−	+	$-m_2\xi'(1-x')\big((\xi'\sqrt{x'(1-x')}k_{2'} + \sqrt{\xi'(1-\xi')}k_{1'})(1-x'-(1-\xi)(1-x))-$ $(\xi\sqrt{x(1-x)}k_2 + \sqrt{\xi(1-\xi)}k_1)(\xi'(1-x'))\big)$
⑦	+	−	+	+	$-m_2\xi(1-x)\big((\xi'\sqrt{x'(1-x')}k_{2'} + \sqrt{\xi'(1-\xi')}k_{1'})(1-x'-(1-\xi)(1-x))-$ $(\xi\sqrt{x(1-x)}k_2 + \sqrt{\xi(1-\xi)}k_1)(\xi'(1-x'))\big)$
⑧	−	+	−	−	$m_2\xi(1-x)\big((\xi'\sqrt{x'(1-x')}k_{2'}^* + \sqrt{\xi'(1-\xi')}k_{1'}^*)(1-x'-(1-\xi)(1-x))-$ $(\xi\sqrt{x(1-x)}k_2^* + \sqrt{\xi(1-\xi)}k_1^*)(\xi'(1-x'))\big)$
⑨	+	+	−	+	$-m_1(1-\xi')(1-x')\big(((1-\xi')\sqrt{x'(1-x')}k_{2'} - \sqrt{\xi'(1-\xi')(1-x')}k_{1'})(\xi(1-x)+x'-1)+$ $((1-\xi)\sqrt{x(1-x)}k_2 - \sqrt{\xi(1-\xi)}k_1)(1-\xi')(1-x')\big)$
⑩	−	−	+	−	$m_1(1-\xi')(1-x')\big(((1-\xi')\sqrt{x'(1-x')}k_{2'}^* - \sqrt{\xi'(1-\xi')(1-x')}k_{1'}^*)(\xi(1-x)+x'-1)+$ $((1-\xi)\sqrt{x(1-x)}k_2^* - \sqrt{\xi(1-\xi)}k_1^*)(1-\xi')(1-x')\big)$
⑪	+	−	−	−	$-m_1(1-\xi)(1-x)\big(((1-\xi')\sqrt{x'(1-x')}k_{2'} - \sqrt{\xi'(1-\xi')(1-x')}k_{1'})(\xi(1-x)+x'-1)+$ $((1-\xi)\sqrt{x(1-x)}k_2 - \sqrt{\xi(1-\xi)}k_1)(1-\xi')(1-x')\big)$
⑫	−	+	+	+	$m_1(1-\xi)(1-x)\big(((1-\xi')\sqrt{x'(1-x')}k_{2'}^* - \sqrt{\xi'(1-\xi')(1-x')}k_{1'}^*)(\xi(1-x)+x'-1)+$ $((1-\xi)\sqrt{x(1-x)}k_2^* - \sqrt{\xi(1-\xi)}k_1^*)(1-\xi')(1-x')\big)$
⑬	+	−	−	+	$m_1 m_2(\xi(1-x)-\xi'(1-x'))((1-\xi)(1-x)-(1-\xi')(1-x'))$
⑭	−	+	+	−	$m_1 m_2(\xi(1-x)-\xi'(1-x'))((1-\xi)(1-x)-(1-\xi')(1-x'))$
⑮	+	+	−	−	0
⑯	−	−	+	+	0

3.4 Outlook

In this thesis, we developed a generalization of BLFQ based on previous work on the two-body system. In the phenomenological point of view, our generalization shares similar functional forms with those two-body systems; on the other hand, we provide initial results of our model and compare with experimental data.

The BLFQ approach is likely to be better at describing heavy systems than light systems. Thus a possible way to extent the current work is to test heavy baryon systems. It could also be extended to higher Fock sectors, for example, the one gluon emission and absorption terms could be added and numerically diagonalized to split the degeneracy in the transverse direction. There is no intrinsic difference between the one gluon exchange formalism of mesons and baryons, but the additional layers of integration and numerical calculations have to be carefully implemented. Once the full LFWFs has been obtained, this model can be augmented by spin in order to be capable to calculate many other observables. Symmetrization of this model should be explored, a possible route is using the inverse Jacobi transformation on LFWF to find wave functions in single particle coordinates, symmetrize the wave functions then transform back. Another possible route would be trying other possible coordinate transformations which separate the center of mass kinetic energy, which has been fully studied in [25]. It is hoped that the convenient basis representations and confining Hamiltonian presented here will stimulate these additional lines of investigation.

BIBLIOGRAPHY

[1] V.I. Arnol'd. *Mathematical methods of classical mechanics*, volume 60. Springer Science & Business Media, 2013.

[2] M. Srednicki. *Quantum field theory*. Cambridge University Press, 2007.

[3] S.J. Brodsky, H.-C. Pauli, and S.S. Pinsky. Quantum chromodynamics and other field theories on the light cone. *Physics Reports*, 301(4):299 – 486, 1998.

[4] N. Brambilla, S. Eidelman, B.K. Heltsley, R. Vogt, G.T. Bodwin, E. Eichten, A.D. Frawley, A.B. Meyer, R.E. Mitchell, V. Papadimitriou, P. Petreczky, A.A. Petrov, P. Robbe, A. Vairo, A. Andronic, R. Arnaldi, P. Artoisenet, G. Bali, A. Bertolin, D. Bettoni, J. Brodzicka, G. E. Bruno, A. Caldwell, J. Catmore, C.-H. Chang, K.-T. Chao, E. Chudakov, P. Cortese, P. Crochet, A. Drutskoy, U. Ellwanger, P. Faccioli, A. Gabareen Mokhtar, X. Garcia i Tormo, C. Hanhart, F.A. Harris, D. M. Kaplan, S. R. Klein, H. Kowalski, J.-P. Lansberg, E. Levichev, V. Lombardo, C. Lourenço, F. Maltoni, A. Mocsy, R. Mussa, F. S. Navarra, M. Negrini, M. Nielsen, S. L. Olsen, P. Pakhlov, G. Pakhlova, K. Peters, A.D. Polosa, W. Qian, J.-W. Qiu, G. Rong, M.A. Sanchis-Lozano, E. Scomparin, P. Senger, F. Simon, S. Stracka, Y. Sumino, M. Voloshin, C. Weiss, H.K. Wöhri, and C.-Z. Yuan. Heavy quarkonium: progress, puzzles, and opportunities. *The European Physical Journal C*, 71(2):1534, Feb 2011.

[5] T. Appelquist, R. Barnett, and K. Lane. Charm and beyond. *Annual Review of Nuclear and Particle Science*, 28(1):387–499, 1978.

[6] N. Brambilla, A. Pineda, J. Soto, and A. Vairo. Effective-field theories for heavy quarkonium. *Rev. Mod. Phys.*, 77:1423–1496, Dec 2005.

[7] M. Neubert. Heavy-quark symmetry. *Physics Reports*, 245(5):259 – 395, 1994.

[8] S. Godfrey and N. Isgur. Mesons in a relativized quark model with chromodynamics. *Phys. Rev. D*, 32:189–231, Jul 1985.

[9] S.J. Brodsky, G.F. de Téramond, H.G. Dosch, and J. Erlich. Light-front holographic qcd and emerging confinement. *Physics Reports*, 584:1 – 105, 2015. Light-front holographic QCD and emerging confinement.

[10] Y. Li, P. Maris, X. Zhao, and J.P. Vary. Heavy quarkonium in a holographic basis. *Phys. Lett. B*, 758(Supplement C):118 – 124, 2016.

[11] M. Krautgärtner, H.C. Pauli, and F. Wölz. Positronium and heavy quarkonia as testing case for discretized light-cone quantization. *Phys. Rev. D*, 45:3755–3774, May 1992.

[12] S. Tang, Y. Li, P. Maris, and J. P. Vary. B_c mesons and their properties on the light front. *Phys. Rev. D*, 98:114038, Dec 2018.

[13] Y. Li, P. Maris, and J.P. Vary. Quarkonium as a relativistic bound state on the light front. *Phys. Rev. D*, 96:016022, Jul 2017.

[14] Meijian Li, Yang Li, Pieter Maris, and James P. Vary. Radiative transitions between 0^{-+} and 1^{--} heavy quarkonia on the light front. *Phys. Rev. D*, 98:034024, Aug 2018.

[15] Meijian Li, Yang Li, Pieter Maris, and James P. Vary. Frame dependence of transition form factors in light-front dynamics. *Phys. Rev. D*, 100:036006, Aug 2019.

[16] M. Tanabashi, K. Hagiwara, K. Hikasa, K. Nakamura, Y. Sumino, F. Takahashi, J. Tanaka, K. Agashe, G. Aielli, C. Amsler, M. Antonelli, D. M. Asner, H. Baer, Sw. Banerjee, R. M. Barnett, T. Basaglia, C. W. Bauer, J. J. Beatty, V. I. Belousov, J. Beringer, S. Bethke, A. Bettini, H. Bichsel, O. Biebel, K. M. Black, E. Blucher, O. Buchmuller, V. Burkert, M. A. Bychkov, R. N. Cahn, M. Carena, A. Ceccucci, A. Cerri, D. Chakraborty, M.-C. Chen, R. S. Chivukula, G. Cowan, O. Dahl, G. D'Ambrosio, T. Damour, D. de Florian, A. de Gouvêa, T. DeGrand, P. de Jong, G. Dissertori, B. A. Dobrescu, M. D'Onofrio, M. Doser, M. Drees, H. K. Dreiner, D. A. Dwyer, P. Eerola, S. Eidelman, J. Ellis, J. Erler, V. V. Ezhela, W. Fetscher, B. D. Fields, R. Firestone, B. Foster, A. Freitas, H. Gallagher, L. Garren, H.-J. Gerber, G. Gerbier, T. Gershon, Y. Gershtein, T. Gherghetta, A. A. Godizov, M. Goodman, C. Grab, A. V. Gritsan, C. Grojean, D. E. Groom, M. Grünewald, A. Gurtu, T. Gutsche, H. E. Haber, C. Hanhart, S. Hashimoto, Y. Hayato, K. G. Hayes, A. Hebecker, S. Heinemeyer, B. Heltsley, J. J. Hernández-Rey, J. Hisano, A. Höcker, J. Holder, A. Holtkamp, T. Hyodo, K. D. Irwin, K. F. Johnson, M. Kado, M. Karliner, U. F. Katz, S. R. Klein, E. Klempt, R. V. Kowalewski, F. Krauss, M. Kreps, B. Krusche, Yu. V. Kuyanov, Y. Kwon, O. Lahav, J. Laiho, J. Lesgourgues, A. Liddle, Z. Ligeti, C.-J. Lin, C. Lippmann, T. M. Liss, L. Littenberg, K. S. Lugovsky, S. B. Lugovsky, A. Lusiani, Y. Makida, F. Maltoni, T. Mannel, A. V. Manohar, W. J. Marciano, A. D. Martin, A. Masoni, J. Matthews, U.-G. Meißner, D. Milstead, R. E. Mitchell, K. Mönig, P. Molaro, F. Moortgat, M. Moskovic, H. Murayama, M. Narain, P. Nason, S. Navas, M. Neubert, P. Nevski, Y. Nir, K. A. Olive, S. Pagan Griso, J. Parsons, C. Patrignani, J. A. Peacock, M. Pennington, S. T. Petcov, V. A. Petrov, E. Pianori, A. Piepke, A. Pomarol, A. Quadt, J. Rademacker, G. Raffelt, B. N. Ratcliff, P. Richardson, A. Ringwald, S. Roesler, S. Rolli, A. Romaniouk, L. J. Rosenberg, J. L. Rosner, G. Rybka, R. A. Ryutin, C. T. Sachrajda, Y. Sakai, G. P. Salam, S. Sarkar, F. Sauli, O. Schneider, K. Scholberg, A. J. Schwartz, D. Scott, V. Sharma, S. R. Sharpe, T. Shutt, M. Silari, T. Sjöstrand, P. Skands, T. Skwarnicki, J. G. Smith, G. F. Smoot, S. Spanier, H. Spieler, C. Spiering, A. Stahl, S. L. Stone, T. Sumiyoshi, M. J. Syphers, K. Terashi, J. Terning, U. Thoma, R. S. Thorne, L. Tiator, M. Titov, N. P. Tkachenko, N. A. Törnqvist, D. R. Tovey, G. Valencia, R. Van de Water, N. Varelas, G. Venanzoni, L. Verde, M. G. Vincter, P. Vogel, A. Vogt, S. P. Wakely, W. Walkowiak, C. W. Walter, D. Wands, D. R. Ward, M. O. Wascko, G. Weiglein, D. H. Weinberg, E. J. Weinberg, M. White, L. R. Wiencke, S. Willocq, C. G. Wohl, J. Womersley, C. L. Woody, R. L. Workman, W.-M. Yao, G. P. Zeller, O. V. Zenin, R.-Y. Zhu, S.-L. Zhu, F. Zimmermann, P. A. Zyla, J. Anderson, L. Fuller, V. S. Lugovsky, and P. Schaffner. Review of particle physics. *Phys. Rev. D*, 98:030001, Aug 2018.

[17] S.D. Drell, D.J. Levy, and T.-M. Yan. A field-theoretic model for electron-nucleon deep inelastic scattering. *Phys. Rev. Lett.*, 22:744–749, Apr 1969.

[18] J.R. Hiller. Nonperturbative light-front hamiltonian methods. *Progress in Particle and Nuclear Physics*, 90:75 – 124, 2016.

[19] S.J. Brodsky and S.D. Drell. Anomalous magnetic moment and limits on fermion substructure. *Phys. Rev. D*, 22:2236–2243, Nov 1980.

[20] J.J. Murphy, Y.M. Shin, and D.M. Skopik. Proton form factor from 0.15 to 0.79 fm^{-2}. *Phys. Rev. C*, 9:2125–2129, Jun 1974.

[21] F. Borkowski, G.G. Simon, V.H. Walther, and R.D. Wendling. Electromagnetic form factors of the peoton at low four-momentum transfer (II). *Nuclear Physics B*, 93(3):461 – 478, 1975.

[22] Ch. Berger, V. Burkert, G. Knop, B. Langenbeck, and K. Rith. Electromagnetic form factors of the proton at squared four-momentum transfers between 10 and 50 fm^{-2}. *Physics Letters B*, 35(1):87 – 89, 1971.

[23] R.C. Walker, B. W. Filippone, J. Jourdan, R. Milner, R. McKeown, D. Potterveld, L. Andivahis, R. Arnold, D. Benton, P. Bosted, G. deChambrier, A. Lung, S. E. Rock, Z.M. Szalata, A. Para, F. Dietrich, K. Van Bibber, J. Button-Shafer, B. Debebe, R.S. Hicks, S. Dasu, P. de Barbaro, A. Bodek, H. Harada, M. W. Krasny, K. Lang, E.M. Riordan, R. Gearhart, L.W. Whitlow, and J. Alster. Measurements of the proton elastic form factors for $1 \leq Q^2 \leq 3$ $(\mathrm{GeV}/c)^2$ at SLAC. *Phys. Rev. D*, 49:5671–5689, Jun 1994.

[24] W. Bartel, F.-W. Büsser, W.-R. Dix, R. Felst, D. Harms, H. Krehbiel, P.E. Kuhlmann, J. McElroy, J. Meyer, and G. Weber. Measurement of proton and neutron electromagnetic form factors at squared four-momentum transfers up to 3 $(\mathrm{GeV}/c)^2$. *Nuclear Physics B*, 58(2):429 – 475, 1973.

[25] L. Fortunato. All transformations of coordinates that separate the center of mass kinetic energy, their group structure and geometry. *Journal of Physics A: Mathematical and Theoretical*, 43(6):065301, jan 2010.

[26] Paul Wiecki, Yang Li, Xingbo Zhao, Pieter Maris, and James P Vary. Non-perturbative calculation of the positronium mass spectrum in basis light-front quantization. *Few-Body Systems*, 56(6-9):489–494, 2015.

[27] L Chaos-Cador and E Ley-Koo. Common generating functions of complete harmonic oscillator wave functions and transformation brackets in d dimensions. *International journal of quantum chemistry*, 97(4):844–853, 2004.

APPENDIX A. A GENERALIZED JACOBI TRANSFORMATION

We have seen how Jacobi coordinates and momenta are fitted in the framework of BLFQ when dealing with mesons and baryons. A follow-up question to ask is whether it is possible to generalize our usage of Jacobi coordinates and momenta in other many-particle systems; if we could, can we incorporate longitudinal confinement into our framework as well? For example: if we want to study a system with 2 quarkonium pairs, do we combine those quarks one by one as we have seen in previous chapters or do we implement the systems of quarkonium pairs; and how we come up with a appropriate longitudinal confining potential? For solving this issue, and preparing for future study, we provide one possible generalization. We shall start with a general setup, then dive into light-front world.

Let's take a look at the case of 2 quarkonium pairs again to see if we can develop some insight. We could combine the quarks inside quarkonia pair first then put the quarkonia together. In other words, we treat the quarkonium as a cluster, then we could use the 2-body Jacobi coordinates and momenta inside the cluster. Finally, we want to treat those clusters as particles and we want to deal with those "particles" in the way we have done in 2-body system. This idea leads us to generalize Jacobi coordinates as follows: we separate the system in different clusters, and those clusters might contain one or more particles. We find the "local" Jacobi coordinates in each cluster and then we define "cluster" Jacobi coordinates for different clusters.

We now express this idea in a formal way: suppose we divide an N-body system to n clusters in which the i-th cluster contains l_i particles. It is convenient to define following quantities

- x_{ij}: the "global" weight of j-th particle in i-th cluster,
- $X_{ij} = \sum_{k=1}^{j} x_{ik}$, $x_i = \sum_{j=1}^{l_i} x_{ij}$, $X_i = \sum_{k=1}^{i} x_k$,
- y_{ij}: the "local" weight of j-th particle in i-th cluster, i.e., $y_{ij} = x_{ij}/x_i$,

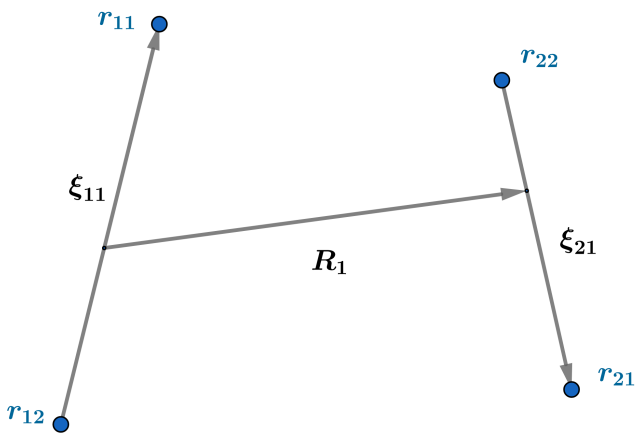

Figure A.1 A possible set of generalized Jacobi coordinates for quarkoniums pair, i.e., four-body system. The labels on the blue dots signify the single particle coordinates while arrows presented are the generalized Jacobi coordinates.

- $Y_{ij} = \sum_{k=1}^{j} y_{ik}$,
- $\boldsymbol{r}_i = \sum_{j=1}^{l_i} y_{ij}\boldsymbol{r}_{ij}$, $\boldsymbol{p}_i = \sum_{j=1}^{l_i} \boldsymbol{p}_{ij}$.

We construct $\xi_{ij},\ j = 1, 2, \ldots, l_i - 1$ in the usual manner:

$$\boldsymbol{\xi}_{ij} = \frac{1}{Y_{ij}} \sum_{k=1}^{j} y_{ik}\boldsymbol{r}_{ik} - \boldsymbol{r}_{i,j+1}, \tag{A.1}$$

where $\boldsymbol{\xi}_{il_i}$ is defined exactly the same way in the usual Jacobi coordinates sense, i.e., $\boldsymbol{\xi}_{il_i} = \boldsymbol{r}_i$. Then we define "cluster Jacobi coordinates" $\boldsymbol{R}_i,\ i = 1, 2, \ldots, n - 1$ as:

$$\boldsymbol{R}_i = \frac{1}{X_i} \sum_{k=1}^{i} x_k\boldsymbol{r}_k - \boldsymbol{r}_{i+1}, \tag{A.2}$$

written explicitly, we have

$$\begin{cases} \boldsymbol{R}_1 = \boldsymbol{r}_1 - \boldsymbol{r}_2 = \frac{1}{X_1}\sum_{k=1}^{l_1} x_{1k}\boldsymbol{r}_{1k} - \sum_{k=1}^{l_2} y_{2k}\boldsymbol{r}_{2k} \\ \vdots \\ \boldsymbol{R}_i = \frac{1}{X_i}\left(\sum_{k=1}^{i} x_k\boldsymbol{r}_k\right) - \boldsymbol{r}_{i+1} = \frac{1}{X_i}\left(\sum_{s=1}^{i}\sum_{t=1}^{l_s} x_{st}\boldsymbol{r}_{st}\right) - \sum_{k=1}^{l_{i+1}} y_{i+1,k}\boldsymbol{r}_{i+1,k} \\ \vdots \\ \boldsymbol{R}_{n-1} = \frac{1}{X_{n-1}}\left(\sum_{k=1}^{n-1} x_k\boldsymbol{r}_k\right) - \boldsymbol{r}_n = \frac{1}{X_{n-1}}\left(\sum_{s=1}^{n-1}\sum_{t=1}^{l_s} x_{st}\boldsymbol{r}_{st}\right) - \sum_{k=1}^{l_n} y_{n,k}\boldsymbol{r}_{n,k} \\ \boldsymbol{R} := \boldsymbol{R}_n = \sum_{k=1}^{n} x_k\boldsymbol{r}_k = \sum_{i,j} x_{ij}\boldsymbol{r}_{ij} \end{cases} . \tag{A.3}$$

Similarly, we construct $q_{ij},\ j = 1, 2, \ldots, l_i - 1$ as:

$$\boldsymbol{q}_{ij} = \frac{1}{Y_{i,j+1}}\left(y_{i,j+1}\sum_{k=1}^{j}\boldsymbol{p}_{ik} - Y_{ij}\boldsymbol{p}_{i,j+1}\right), \tag{A.4}$$

and define "cluster Jacobi momentum" $\boldsymbol{P}_i,\ i = 1, 2, \ldots, n-1$ as

$$\boldsymbol{P}_i = \frac{1}{X_{i+1}}\left(x_{i+1}\sum_{k=1}^{i}\boldsymbol{p}_k - X_i\boldsymbol{p}_{i+1}\right) \tag{A.5}$$

where they satisfy commutation relation

$$[q_{ij}^a, R_k^b] = 0,\ [\xi_{ij}^a, P_k^b] = 0,\ [\xi_{ij}^a, q_{lm}^b] = i\delta_{ab}\delta_{il}\delta_{jm},\ [R_i^a, P_j^b] = i\delta_{ab}\delta_{ij}. \tag{A.6}$$

We see indeed $\{\xi_{ij}, R_k\}$ and $\{q_{ij}, P_k\}$ are canonical conjugate pairs.

APPENDIX B. BASIS HAMILTONIAN IN A GENERAL SETTING

The transverse Hamiltonian

$$H_{\rm T} = T_{\rm T} + V_{\rm T} = \left(\sum_{i=1}^{n} \sum_{j=1}^{l_i} \frac{\boldsymbol{p}_{ij\perp}^2}{x_{ij}} - \boldsymbol{P}_\perp^2 \right) + \kappa^4 \left(\sum_{i=1}^{n} \sum_{j=1}^{l_i} x_{ij} \boldsymbol{r}_{ij\perp}^2 - \boldsymbol{R}_\perp^2 \right) \tag{B.1}$$

is diagonal quadratic under the generalized Jacobi coordinates and momenta. We rewrite the reduced kinetic energy $T_{\rm T}$ as

$$T_{\rm T} = \sum_{i=1}^{n} \left(\sum_{j=1}^{l_i} \frac{\boldsymbol{p}_{ij\perp}^2}{x_{ij}} - \frac{\boldsymbol{p}_{i\perp}^2}{x_i} \right) + \sum_{i=1}^{n} \frac{\boldsymbol{p}_{i\perp}^2}{x_i} - \boldsymbol{P}_\perp^2, \tag{B.2}$$

thanks to Eq.(2.33), each fixed i inside the parenthesis is diagonal in its own cluster and the same reasoning applies to the remaining part. Finally, the potential $V_{\rm T}$ is also diagonal due to Eq.(2.37).

The longitudinal confinement $V_{\rm L}$ is defined in a similar manner to Eq.(2.44), let $\gamma_i = x_{i+1}/X_{i+1}$, $\gamma_{ij} = x_{i,j+1}/X_{i,j+1}$ be the relative longitudinal momentum transfer of clusters and particles respectively. We construct $V_{\rm L}$ as

$$V_{\rm L} = -\frac{\kappa^4}{M^2} \left(\sum_{i=1}^{n} \sum_{j=1}^{l_i - 1} \frac{1}{X_{i,j+1}} \partial_{\gamma_{ij}} \left(\gamma_{ij} \left(1 - \gamma_{ij} \right) \partial_{\gamma_{ij}} \right) + \sum_{i=1}^{n-1} \frac{1}{X_{i+1}} \partial_{\gamma_i} \left(\gamma_i \left(1 - \gamma_i \right) \partial_{\gamma_i} \right) \right). \tag{B.3}$$

Combining $V_{\rm L}$ with the mass terms in the light-front kinetic energy gives the longitudinal Hamiltonian $H_{\rm L}$ which is analytically solvable in a recursive fashion whose steps are elaborated shown in Chap.(2.4). Together with $H_{\rm T}$ we will finally obtain a possible BLFQ basis Hamiltonian for any particle system with any cluster assignment, whose eigenfunctions are analytically solvable. These analytic solutions can then be treated as basis states into which additional interactions are introduced and symmetrization (resp. antisymmetrization) among identical bosons (resp. fermions) is managed.

APPENDIX C. DIRAC FORM FACTOR $F_1(q^2)$

The Dirac form factor representation using Eq.(3.4) on our wavefunction is given

$$F_1(q^2) = \pi \int_{[0,1]^2} \mathrm{d}\gamma_1 \mathrm{d}\gamma_2 \sum_{i=1}^{3} e_i \sum_{N_1,N_2} \mathcal{M}^{N_1,0,\mu_1,\nu_1}_{n_1,m_1,n_1,-m_1} \mathcal{M}^{N_2,0,\mu_2,\nu_2}_{n_2,m_2,n_2,-m_2} (-1)^{N_1+N_2} \cdot \phi_{\mu_1,\nu_1}(\frac{\boldsymbol{\Delta}_{i1}}{\sqrt{2}}) \phi_{\mu_2,\nu_2}(\frac{\boldsymbol{\Delta}_{i2}}{\sqrt{2}}) \left(\chi_{\mathrm{L}}^{(A,B)}(\gamma_1)\chi_{1}^{(\alpha_{\mathrm{L}},\beta)}(\gamma_2)\right)^2, \tag{C.1}$$

where $\mathcal{M}^{N,M,N',-M'}_{n,m,n',-m'}$ are the Talmi-Moshinsky coefficients which can be obtained analytically [26, 27]. In particular, at the ground state,

$$F_1(q^2) = C^2 \int_0^1 \int_0^1 \gamma_1^B (1-\gamma_1)^A \gamma_2^\beta (1-\gamma_2)^{\alpha_{1_1}} \left[\sum_i e_i \exp\left\{\frac{-1}{4\kappa^2}\left(\boldsymbol{\Delta}_{i1}^2 + \boldsymbol{\Delta}_{i2}^2\right)\right\}\right] \mathrm{d}\gamma_1 \mathrm{d}\gamma_2, \tag{C.2}$$

where C is the normalized constant in terms of the Beta function $\boldsymbol{B}(x,y)$,

$$C = \frac{1}{\sqrt{\boldsymbol{B}(B+1,A+1)\boldsymbol{B}(\beta+1,\alpha_{1_1}+1)}}, \tag{C.3}$$

e_i is the fractional charge of constituent quarks, $\boldsymbol{\Delta}_{i1}$ and $\boldsymbol{\Delta}_{i2}$ are the holographic momentum transfer when the i-th particle (quark) is struck, which are displayed in Table C.1.

Table C.1 The transferred holographic momenta and the momentum squared of the three constituent quarks.

i	$\boldsymbol{\Delta}_{i1}$	$\boldsymbol{\Delta}_{i2}$	$\boldsymbol{\Delta}_{i1}^2 + \boldsymbol{\Delta}_{i2}^2$
1	$\frac{-x}{\sqrt{\eta_2}}\boldsymbol{q}$	$\frac{-\xi}{\sqrt{\eta_1}}\boldsymbol{q}$	$\left(\frac{x}{1-x} + \frac{\xi}{(1-\xi)(1-x)}\right) q^2$
2	$\frac{-x}{\sqrt{\eta_2}}\boldsymbol{q}$	$\frac{1-\xi}{\sqrt{\eta_1}}\boldsymbol{q}$	$\left(\frac{x}{1-x} + \frac{1-\xi}{\xi(1-x)}\right) q^2$
3	0	$\frac{1-x}{\sqrt{\eta_1}}\boldsymbol{q}$	$\frac{1-x}{\xi(1-\xi)} q^2$

Note that we perform a Jacobi transformation to single-particle momenta in order to obtain the corresponding momentum transfer in terms of holographic momenta.

APPENDIX D. JACOBI DIFFERENTIAL EQUATION

The Jacobi polynomial $J_n^{\alpha,\beta}(x)$ is defined as

$$J_n^{\alpha,\beta}(x) = \frac{1}{2^n}\sum_{k=0}^{n}\binom{n+\alpha}{k}\binom{n+\beta}{n-k}(x-1)^{n-k}(x+1)^k, \tag{D.1}$$

which is the solution of the linear operator

$$\begin{aligned} L_{\alpha,\beta} &= -\left(1-x\right)^{\alpha}\left(1+x\right)^{\beta}\partial_x\left(\left(1-x\right)^{\alpha+1}\left(1+x\right)^{\beta+1}\partial_x\right) \\ &= \left(x^2-1\right)\partial_x^2 + \left[\left(\alpha+\beta+2\right)x+\alpha-\beta\right]\partial_x. \end{aligned} \tag{D.2}$$

on the interval $[-1,1]$ where the eigenvalues are

$$L_{\alpha,\beta}J_n^{\alpha,\beta}\left(x\right) = \lambda_n^{\alpha,\beta}J_n^{\alpha,\beta}\left(x\right), \quad \lambda^{\alpha,\beta} = n\left(n+\alpha+\beta+1\right). \tag{D.3}$$

They are orthogonal with respect to the weight $(1-x)^{\alpha}(1+x)^{\beta}$.

In light-front coordinates, the interval in which longitudinal momentum fractions live in is $[0,1]$. We perform a transformation

$$x \to 2x-1, \tag{D.4}$$

then $x+1 \to 2x,\ 1-x \to 2\left(1-x\right)$ and $\partial_x \to \partial_x/2$. Hence the Jacobi linear operator becomes

$$L_{\alpha,\beta} = x\left(x-1\right)\partial_x^2 + \left[\left(\alpha+\beta+2\right)x-\left(\beta+1\right)\right]\partial_x. \tag{D.5}$$

The longitudinal basis functions are defined as

$$\chi_n^{\alpha,\beta}\left(x\right) = C(1-x)^{\frac{\alpha}{2}}x^{\frac{\beta}{2}}J_n^{\alpha,\beta}(x), \tag{D.6}$$

where C is the normalization factor. To see the relation between the basis functions and effective longitudinal potential, we calculate the following in detail,

$$-\partial_x\left(x\left(1-x\right)\partial_x\left(x^{\frac{\beta}{2}}\left(1-x\right)^{\frac{\alpha}{2}}\right)J_n^{\alpha,\beta}\left(2x-1\right)\right) \overset{\text{def}}{=} -\partial_x\left(x\left(1-x\right)\partial_x\chi_n^{\alpha,\beta}\left(x\right)\right) \overset{\text{def}}{=} \tilde{L}_n^{\alpha,\beta}\chi_n^{\alpha,\beta}\left(x\right)$$

The terms by order of derivatives are

$$\begin{aligned}
T_2 &= x\left(x-1\right)\left(x^{\frac{\beta}{2}}\left(1-x\right)^{\frac{\alpha}{2}}\right)\partial_x^2 J_n^{\alpha,\beta}\left(2x-1\right),\\
T_1 &= -\left[\partial_x\left(x^{\frac{\beta}{2}+1}\left(1-x\right)^{\frac{\alpha}{2}+1}\right)+x\left(1-x\right)\partial_x\left(x^{\frac{\beta}{2}}\left(1-x\right)^{\frac{\alpha}{2}}\right)\right]\partial_x J_n^{\alpha,\beta}\\
&= -\left[\left(\frac{\beta}{2}+1+\frac{\beta}{2}\right)\left(1-x\right)-\left(\frac{\alpha}{2}+1+\frac{\alpha}{2}\right)x\right]\left(x^{\frac{\beta}{2}}\left(1-x\right)^{\frac{\alpha}{2}}\right)\partial_x J_n^{\alpha,\beta}\left(2x-1\right)\\
&= \left[\left(\alpha+\beta+2\right)x-\left(\beta+1\right)\right]\left(x^{\frac{\alpha}{2}}\left(1-x\right)^{\frac{\beta}{2}}\right)\partial_x J_n^{\alpha,\beta}\left(2x-1\right) \qquad \text{(D.7)}\\
T_0 &= -\partial_x\left(x\left(1-x\right)\partial_x\left(x^{\frac{\beta}{2}}\left(1-x\right)^{\frac{\alpha}{2}}\right)\right)J_n^{\alpha,\beta}\left(2x-1\right)\\
&= -\left[\frac{\beta^2}{4}\frac{1-x}{x}+\frac{\alpha^2}{4}\frac{x}{1-x}-\frac{\alpha}{2}(1+\frac{\beta}{2})-\frac{\beta}{2}(1+\frac{\alpha}{2})\right]\chi_n^{\alpha,\beta}\left(x\right)\\
&= \left[\left(\frac{\alpha^2}{4}+\frac{\beta^2}{4}+\frac{\alpha\beta}{2}+\frac{\alpha}{2}+\frac{\beta}{2}\right)-\frac{1}{4}\left(\frac{\beta^2}{x}+\frac{\alpha^2}{1-x}\right)\right]\chi_n^{\alpha,\beta}\left(x\right)
\end{aligned}$$

Combining terms in above equation we obtain

$$\begin{aligned}
\tilde{L}_n^{\alpha,\beta}\chi_n^{\alpha,\beta}\left(x\right) &= -\partial_x\left(x\left(1-x\right)\partial_x\chi_n^{\alpha,\beta}\left(x\right)\right)\\
&= T_0+T_1+T_2\\
&= -\frac{1}{4}\left(\frac{\beta^2}{x}+\frac{\alpha^2}{1-x}\right)\chi_n^{\alpha,\beta}\left(x\right)+\left(\lambda_n^{\alpha,\beta}+\frac{\alpha^2}{4}+\frac{\beta^2}{4}+\frac{\alpha\beta}{2}+\frac{\alpha}{2}+\frac{\beta}{2}\right)\chi_n^{\alpha,\beta}\left(x\right)\\
&= -\frac{1}{4}\left(\frac{\beta^2}{x}+\frac{\alpha^2}{1-x}\right)\chi_n^{\alpha,\beta}\left(x\right)+\left(n+\frac{1}{2}(\alpha+\beta)\right)\left(n+\frac{1}{2}(\alpha+\beta)+1\right)\chi_n^{\alpha,\beta}\left(x\right).
\end{aligned} \qquad \text{(D.8)}$$

So the n-th eigenfunction to the linear operator $-\gamma^2\partial_x\left(x\left(1-x\right)\partial_x\right)+\left(\beta^2/x+\alpha^2/(1-x)\right)$ is

$$\left(x^{\frac{\beta}{\gamma}}\left(1-x\right)^{\frac{\alpha}{\gamma}}\right)J_n^{\frac{2\alpha}{\gamma},\frac{2\beta}{\gamma}}\left(2x-1\right), \qquad \text{(D.9)}$$

with corresponding eigenvalue

$$\begin{aligned}
(n\gamma+\alpha+\beta)((n+1)\gamma+\alpha+\beta) &= (\alpha+\beta)^2+(2n+1)(\alpha+\beta)\gamma+n(n+1)\gamma^2\\
&= \left((n+\frac{1}{2})\gamma+\alpha+\beta\right)^2-\frac{\gamma^2}{4}.
\end{aligned} \qquad \text{(D.10)}$$